UPPSALA
UNIVERSITET

Digital Comprehensive Summaries of Uppsala Dissertations from the Faculty of Science and Technology 1616

Engineering cyanobacteria for increased growth and productivity

FEIYAN LIANG

ACTA
UNIVERSITATIS
UPSALIENSIS
UPPSALA
2018

ISSN 1651-6214
ISBN 978-91-513-0201-0
urn:nbn:se:uu:diva-338081

Dissertation presented at Uppsala University to be publicly examined in Häggsalen, Ang/10132, Ångströmlaboratoriet, Lägerhyddsvägen 1, Uppsala, Friday, 23 February 2018 at 09:15 for the degree of Doctor of Philosophy. The examination will be conducted in English. Faculty examiner: Professor Olaf Kruse (Bielefeld University, Germany).

Abstract

Liang, F. 2018. Engineering cyanobacteria for increased growth and productivity. *Digital Comprehensive Summaries of Uppsala Dissertations from the Faculty of Science and Technology* 1616. 63 pp. Uppsala: Acta Universitatis Upsaliensis. ISBN 978-91-513-0201-0.

Increasing the photosynthetic efficiency is one of the strategies to increase the crop yields to meet the requirement of 50% more food by 2050. Due to the similarity on photosynthesis between crops and cyanobacteria, cyanobacteria are ideal alternatives to study photosynthesis since cyanobacteria are prokaryotes, easier to engineer and have shorter life cycle. On the other hand, cyanobacteria are promising cell factories for food additives, biofuels, and other products. To get the desired products from cyanobacteria directly will consume atmospheric CO_2 and avoid additional releasing of CO_2 from the usage of fossil resources.

In this thesis, four CBB cycle enzymes were overexpressed individually in the model cyanobacterium *Synechocystis* PCC 6803. To get ribulose-1,5-bisphosphate carboxylase/oxygenase (RuBisCO) overexpressed, two methods were used. One was to introduce another copy of the carboxysome protein CcmM gene into the cells since CcmM is essential for packing RuBisCO into the carboxysome. Another way was to tag the RuBisCO gene either on the N terminus of the large subunit or on the C terminus of the small subunit by FLAG. Even though the RuBisCO level increased, the specific RuBisCO activity did not change. Fructose-1,6-/sedoheptulose-1,7-bisphosphatase (FBP/SBPase), aldolase (FBA) and transketolase (TK) were overexpressed by introducing a second copy of corresponding gene. The engineered strains with increased levels of RuBisCO, FBP/SBPase, and FBA grew faster, had higher maximum net oxygen evolution rate and accumulated more biomass when cultivated under 100μmol photons m^{-2} s^{-1} light intensity. The strain carrying more TK showed a chlorotic phenotype but still accumulated more biomass under the same light condition. Four strains with one of the CBB cycle enzymes overexpressed were selected to investigate the effects on ethanol production. Increased ethanol production and ethanol to total biomass rate were observed in the CBB cycle engineered strains. The best strain produced almost 50% ethanol out of the total biomass.

This work shows that overexpressing selected enzymes of the CBB cycle in cyanobacteria resulted in enhanced total biomass accumulation and increased compound (exampled as ethanol) production under certain growth conditions.

Keywords: Cyanobacteria, CBB cycle, growth, biomass, photosynthesis, ethanol

Feiyan Liang, Department of Chemistry - Ångström, Molecular Biomimetics, Box 523, Uppsala University, SE-75120 Uppsala, Sweden.

ISSN 1651-6214
ISBN 978-91-513-0201-0
urn:nbn:se:uu:diva-338081 (http://urn.kb.se/resolve?urn=urn:nbn:se:uu:diva-338081)

A calm and modest life brings more happiness than the pursuit of success combined with constant restlessness.
-Albert Einstein

List of Papers

This thesis is based on the following papers, which are referred to in the text by their Roman numerals.

I. **Liang, F**., Lindblad, P. (2016) Effects of Overexpressing Calvin-Bassham-Benson Cycle Carbon Flux Control Enzymes in the Cyanobacterium *Synechocystis* PCC 6803. *Metabolic Engineering*, 38: 56-64

II. **Liang F**., Lindblad, P. (2017) *Synechocystis* PCC 6803 Overexpressing RuBisCO Grow Faster with Increased Photosynthesis. *Metabolic Engineering Communications*, 4: 19-36

III. Englund, E., **Liang, F**., Lindberg, P. (2016) Evaluation of Promoters and Ribosome Binding Sites for Biotechnological Applications in the Unicellular Cyanobacterium *Synechocystis* sp. PCC 6803. *Scientific Reports*, 6: 36640

IV. **Liang, F**., Englund, E., Lindberg, P., Lindblad, P. (2018) Engineered Cyanobacteria with Enhanced Growth Show Increased Ethanol Production and Higher Biofuel to Biomass Ratio. *Submitted*

V. Miao R, Wegelius A, Durall C, **Liang F**, Khanna N, Lindblad P. (2017) Engineering Cyanobacteria for Biofuel Production. In: Hallenbeck P. (ed) Modern Topics in the Phototrophic Prokaryotes. Environmental and Applied Aspects. Chapter 11: 351-393. Springer International Publishing Switzerland. ISBN: 978-3-319-46259-2

Contents

Abbreviations

3-HP	3-hydroxypropionate
3-HP/4-HB	3-hydroxypropionate/4-hydroxybutyrate
ADH	Alcohol dehydrogenase
ATP	Adenosine triphosphate
CETCH	Crotonyl–CoA/ethylmalonyl-CoA/hydroxybutyryl-CoA
DC/4-HB	Dicarboxylate-4-hydroxybutrrate
DCW	Dry cell weight
E. coli	*Escherichia coli*
EYFP	Enhanced yellow fluorescent protein
FBA	Aldolase
FBP/SBPase	Fructose-1,6/sedoheptulose-1,7-bisphosphatase
FBPase	Fructose-1,6-bisphosphatase
GAP	Glyceraldehyde 3-phosphate
GAPDH	Glyceraldehyde 3-phosphate dehydrogenase
MOG	Malonyl-CoA-oxaloacetate-glyoxylate
NAD(P)H	Reduced form of nicotinamide adenine dinucleotide (phosphate)
$NAD(P)^+$	Nicotinamide adenine dinucleotide (phosphate)
OD_{750}	Optical density at 750nm wavelength
OPP	Oxidative pentose phosphate
PDC	Pyruvate decarboxylase
PGA	3-phosphoglycerate
PRK	Phosphoribulokinase
Rca	RuBisCO activase
RLP	RuBisCO like protein
RT-PCR	Reverse transcription polymerase chain reaction
rTCA cycle	Reductive tricarboxylic acid cycle
RuBisCO	Ribulose-1,5-bisphosphate carboxylase/oxygenase
RuBP	Ribulose 1,5-bisphosphate
SBPase	Sedoheptulose-1,7-bisphosphatase
SDS-PAGE	Sodium dodecyl sulfate polyacrylamide gel electrophoresis
Synechocystis	*Synechocystis* PCC 6803
The CBB cycle	The Calvin-Benson-Bassham cycle
TK	Transketolase
TPP	Thiamine pyrophosphate
TRX	Thioredoxin

5’UTR	5’ untranslated region
AAA+	ATPase associated with various cellular activities
CA1P	2-carboxy-D-arabinitol-1-phosphate
CAM	Crassulacean acid metabolism
CCM	Carbon concentration mechanims
DHAP	Dihydroxyacetone phosphate
DPO	Dissimilatory phosphite oxidattion
E4P	Erythrose-4-phosphate
F6P	Fructose-6-phosphate
FBP	Fructose-1,6-bisphosphate
Fd	Ferredoxin
GDH	Glutamate dehydrogenase
GST	Glutathione-S-transferase
HEPES	4-(2-hydroxyethyl)-1-piperazineethanesulfonic acid
MBP	Maltose-binding protein
MTA	5-methylthiopenty
PDBP	2,3-pentodiulose-1,5-bisphosphate
PEPc	Phosphoenolpyruvate carboxylase
R5P	Ribose-5-phosphate
Ru5P	Ribulose-5-phosphate
S7P	Sedoheptulose-7-phosphate
SBP	Sedoheptulose-1,7-bisphosphate
Xu5P	Xylulose-5-phosphate
XuBP	Xylulose-1,5-bisphosphate
TLA	Truncated light-harvesting antenna

Introduction

By 2050, the world population is predicted to increase by more than 30% compared to 2015[1] and the food requirement will increase by 50% because of this and increased daily consumption per individual[2]. It is impossible to produce so much food to meet the demand only by expanding the arable lands. Besides, the energy used nowadays is mainly the fossil fuels, which are organic organisms buried and dehydrated for millions of years. There are increasing restrictions to use the fossil fuels due to the environment pollution it is causing, no regeneration, and uneven distribution. Therefore, increasing the crop yield and finding alternatives to the fossil fuels are two of the major tasks the society is facing.

To solve the two tasks, we have to learn the processes forming fossil fuels and food. Originally, they are mainly from the oxygenic photosynthetic process, which includes the light reaction and the dark reaction (the Calvin-Benson-Bassham, CBB cycle). Generally, in the light reaction, the solar energy is absorbed and converted into ATP. During this process, water is split, oxygen is released and NADPH is formed. In the dark reaction, CO_2 is assimilated consuming ATP and NADPH to synthesize organic compounds.

Cyanobacteria are ancient organisms which appeared long time before the multicellular oxygen consuming lives. Most cyanobacteria, except *Melainabacteria* and *Sericytochromatia*[3], are endowed with oxygenic photosynthesis and contributed to the "Great Oxidation Event", which happened about 2.3 to 2.5 billion years ago[4,5]. The "Great Oxidation Event" changed the atmosphere content from no oxygen to about 21%, which is crucial for the emergence of aerobic lives, human included. In plants, oxygenic photosynthesis occurs in the chloroplast, the compartment descended from cyanobacteria via endosymbiosis[6]. Oxygenic photosynthesis in plant shares high similarities with that in cyanobacteria. However, cyanobacteria have advantages over plants, such as shorter life cycle, simpler and more mature genetic engineering tools, and shorter engineering period. Because of these advantages, cyanobacteria are ideal organisms to study oxygenic photosynthesis and to give guidance on how to increase e.g. crop yield. Besides, cyanobacteria contain specialized carbon concentration mechanisms (CCMs[7]) that may also help to increase crop yield since low CO_2 concentration in the vicinity of ribulose-1, 5-bisphosphate carboxylase/oxygenase (RuBisCO) is one of the bottlenecks in oxygenic photosynthesis[8,9].

In this thesis, I used the model cyanobacterium *Synechocystis* PCC 6803[10] as the host to study the effects of engineering the CBB cycle (the dark reaction) on growth and desired compound production (exampled as ethanol). Experimentally, the expression of four carbon flux control enzymes in the CBB cycle was increased individually, RuBisCO, fructose-1,6/sedoheptulose-1,7-bisphosphatase (FBP/SBPase), aldolase (FBA) and transketolase (TK). The engineered strains grew faster and/or accumulated more biomass under certain laboratory cultivation conditions and produced more ethanol after an ethanol synthesis pathway (Fig. 1) was introduced into the CBB cycle engineered strains. Conclusively speaking, the desired compound yield can be increased by engineering the primary carbon fixation pathway, the CBB cycle, in cyanobacteria.

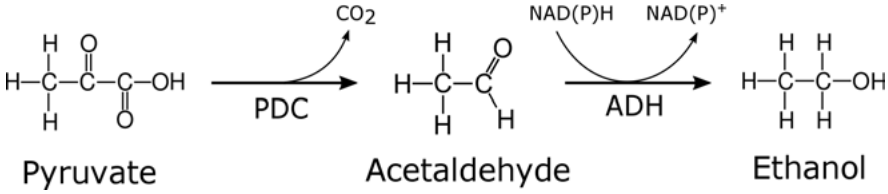

Figure 1. The ethanol synthesis pathway introduced into *Synechocystis* PCC 6803. PDC, pyruvate decarboxylase (the gene used in this thesis is *pdc* from *Zymomonas mobilis*); ADH, alcohol dehydrogenase (the gene used in this thesis is *slr1192* from *Synechocystis* PCC 6803).

The Calvin-Benson-Bassham (CBB) cycle

The CBB cycle, employing RuBisCO to fix CO_2, is the major carbon fixation pathway in nature. It consists of 13 reactions catalyzed by 11 enzymes (Fig. 2). The entire cycle can be divided into 3 stages: (i) ribulose 1, 5-bisphosphate (RuBP) carboxylation, (ii) 3-phosphoglycerate (PGA) reduction, and (iii) RuBP regeneration. In the carboxylation stage, atmospheric CO_2 is incorporated to RuBP and two molecules of PGA are formed. In the reduction stage, the PGA is converted into glyceraldehyde-3-phosphate (GAP), consuming ATP and NADPH from the light reaction. In the regeneration stage, RuBP is reproduced from GAP through several steps. To overview the CBB cycle, the fixation of three molecules of CO_2, which means the generation of one molecule of GAP, requires nine molecules of ATP and six molecules of NADPH. However, the ATP efficiency is lower in reality because of the existence of photorespiration. Photorespiration is that RuBisCO takes O_2 as substrate instead of CO_2 and produces PGA and 2-phosphoglycolate. 2-phosphoglycolate is toxic to the cells. The elimination of 2-phosphoglycolate releases one molecule of fixed carbon for every two molecules of 2-phosphoglycolate, thus reducing the energy efficiency of the CBB cycle.

Even though there are high similarities in the CBB cycle between plants and cyanobacteria, there are still several specificities for the cyanobacterial CBB cycle. In cyanobacteria, RuBisCO is located in a permeable multiunit proteinaceous compartment, carboxysome[11], together with carbonic anhydrase, which coverts bicarbonate into RuBisCO's substrate CO_2. Carboxysome biogenesis was elucidated in a freshwater cyanobactierium *Synechococcus elongatus* PCC 7942[12]. At the beginning of carboxysome biogenesis, the carboxysome protein CcmM, both the long version and the short version[13], aggregates with RuBisCO, forming procarboxysome. This process relies on the binding between RuBisCO small unit like domain of CcmM and RuBisCO. CcmM then binds to the carbonic anhydrase and another carboxysome protein CcmN, whose C-terminus encapsulation peptide binds with the main shell protein CcmK2. Afterwards, the remaining shell proteins are able to join and a functional carboxysome is assembled. Another difference from the plants is that cyanobacteria lack compartments; therefore, the cyanobacterial CBB cycle partially overlaps with the oxidative pentose phosphate (OPP) pathway, the main NADPH supplier under heterotrophic growth conditions. However, the catalytic directions of the CBB cycle and the OPP pathway are opposite. Besides, there are three steps are specific in the CBB cycle and not present in the OPP pathway. The three steps are (i) converting RuBP and CO_2 to PGA by RuBisCO (consumption of RuBP), (ii) phosphorylating ribulose-5-phosphate (Ru5P) to RuBP by phosphoribulokinase (PRK, regeneration of RuBP) and (iii) dephosphorylating sedoheptulose-1,7-bisphosphate (SBP) into sedoheptulose-7-phosphate (S7P) by the bi-functional enzyme FBP/SBPase, which in plants is catalyzed by SBPase. RuBisCO and PRK are also regarded as characteristic enzymes of the CBB cycle.

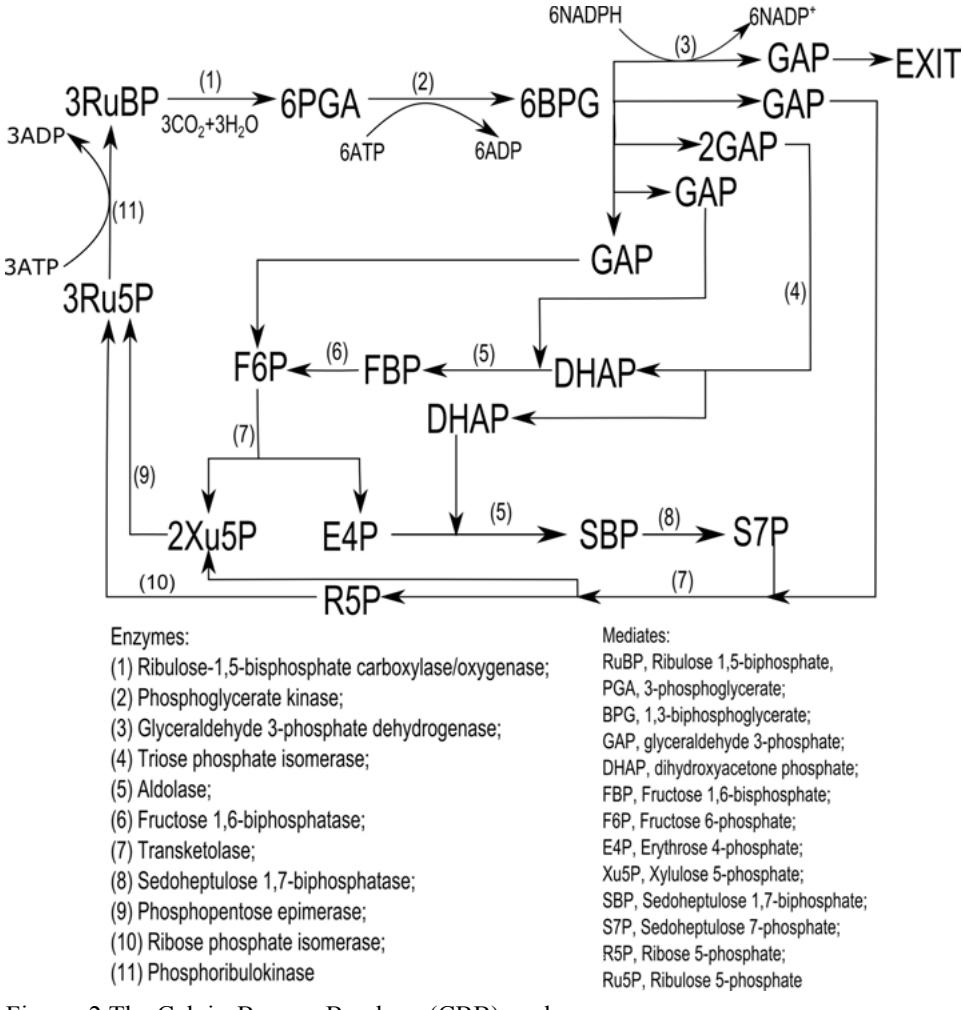

Figure. 2 The Calvin-Benson-Bassham (CBB) cycle.

In the CBB cycle, PRK, glyceraldehyde 3-phosphate dehydrogenase (GAPDH), FBPase and SBPase are the four plant enzymes that have been intensively studied as the redox regulation targets. They are activated by thioredoxin (TRX, mainly f-type TRX), which receives electrons from water splitting in the light reaction through ferredoxin (Fd) and transfers the electrons to the cysteine residue(s) of the target enzymes (ferredoxin/thioredoxin system)[14,15]. Therefore, all four enzymes are light dependent. However, through proteomic studies, it is now believed that not only the four enzymes but all the enzymes in the CBB cycle are redox regulated, via cysteine disulfide reduction or other post-translational modifications, such as glutathionylation, sulfenylation, nitrosylation or combined modifications[16]. Sometimes, the regulation is not direct but through another enzyme. For example, in cyanobacteria and most algae, even though the photosynthetic GAPDH

lacks cysteine residues and the corresponding regulatory domains, it is still regulated by TRX. The mechanism for this regulation is that GAPDH, CP12 and PRK form a supermolecular complex when the TRX is oxidized and the NAD(P)H/NAD(P) ratio is low. In the supermolecular, PRK has the TRX regulation target, cysteine residue so the supermolecular complex is kinetically inhibited in darkness[17–19].

The analysis of redox regulations, together with the other catalytic features of the enzymes, may give some hints of the rate-limiting steps in the CBB cycle. For example, the reaction catalyzed by RuBisCO is irreversible and RuBisCO has slow turnover rate. Therefore, RuBisCO is believed to be one of the bottlenecks. Apart from this, metabolic control analysis is another way to identify the potential rate-limiting steps. In metabolic control analysis, the "flux control co-efficient" is determined by calculating the ratio between the change of flux and the change of specific enzyme activity under certain growth conditions[20]. The value varies between 0 (no control) to 1 (full control). In most cases, the full control is excreted by several enzymes and one of the enzymes may play a critical role. Earlier results in plants indicated that RuBisCO, SBPase (FBP/SBPase in cyanobacteria), FBA and TK have main controls over the carbon fixation flux under certain growth conditions[8,9]. Among the four enzymes, RuBisCO catalyzes the carboxylation of RuBP, while the other three enzymes catalyze reactions during the RuBP regeneration stage.

Ribulose-1, 5-bisphosphate carboxylase/oxygenase (RuBisCO)

In the CBB cycle, RuBisCO (EC 4.1.1.39) incorporates one molecule of CO_2 with the RuBP and cleaves the unstable intermediate into two molecules of PGA. This is the predominant way for atmospheric CO_2 entering the biological cycle and it is responsible for more than 90% of the carbon fixed into biomass. RuBisCO started to evolve about 3.8 billion years ago when its substrate CO_2 was the dominant atmospheric gas. After that, it further evolved following restrictions between biochemical constraint and evolution pressure[21], carboxylation velocity and CO_2 affinity[22], and holoenzyme stability and activity as the atmospheric gas content changed dramatically[23]. During the evolution of RuBisCO, the photoautotrophic organisms developed different characteristics to maximize the net photosynthetic efficiency adapted to the habitation conditions. For example, in C3 plants, RuBisCO is abundant, around quarter of the soluble proteins in leaves, and consumes almost half of the nitrogen sources. In C4 and crassulacean acid metabolism (CAM) plants, carbon fixation process uses a relatively efficient carboxylase phosphoenolpyruvate carboxylase (PEPc) to fix atmospheric CO_2 into a C4 acid. The C4 acid will later release CO_2 near RuBisCO to increase the substrate concentration. Their carbon fixation processes consist of reactions in different cells (C4 plants) or under day/night cycles (CAM plants)[24]. In

aquatic green algae and cyanobacteria, special proteinaceous compartments are developed (pyrenoid in green algae and hornworts and carboxysome in cyanobacteria) to increase the CO_2 concentration in the vicinity of RuBisCO since CO_2 diffuses 10000 times slower in water than in air[25,26]. Accordingly, carboxylation velocity and CO_2 affinity of RuBisCO differ from different organisms. For instant, RuBisCO from C3 plants (without carbon concentrating mechanisms) has relatively higher CO_2 affinity and lower carboxylation velocity compared to RuBisCO from organisms with carbon concentrating mechanisms (C4 plants, CAM plants, hornworts, green algae and cyanobacteria)[27]. Because of this, cross-species RuBisCO expression, e.g. overexpressing cyanobacterial RuBisCO in plants[28], is one of the promising strategies to increase RuBisCO performance in target organisms. However, this effort is usually restricted by e.g. the differences on folding and assembling chaperones[29,30].

There are four forms of RuBisCO reported, I to IV[31]. Cyanobacteria, proteobacteria, algae and plants possess form I RuBisCO, which is the most common form in nature. It is a hexadecameric holoenzyme consisting of eight large subunits in the form of $4(L_2)$ and eight small subunits with four on each end of the large subunits core $4(L_2)$. The antiparallel dimer L_2 is essential for catalytic activity since the catalytic site consists of the N-terminal domain of one large subunit and the C-terminal domain of the other large subunit in the dimer. Therefore, there are two catalytic sites in each dimer. The small subunit is not essential for the catalytic activity, but it may stabilize and concentrate the large subunits dimers and contribute to CO_2/O_2 specificity[32]. Form II RuBisCO only contains one or more L_2, without small subunits. Form III RuBisCO, which only exits in Archaea, also lacks small subunits and has three to five L_2 to form a ring structure. However, a complete CBB cycle is not found in Archaea and the form III RuBisCO does not support autotrophic growth. Form IV RuBisCO, a RuBisCO like protein (RLP), is different from the former three forms since it lacks the conserved residues in the active sites and does not have the carboxylase and oxygenase activity[33]. Functions of RLPs are not identical in different organisms. For example, in *Chlorobium tepidum*, RLP is related to oxidative stress response and sulfur utilization[34]. In *Bacillus subtilis* and *Rhodospirillum rubrum*, RLP is to remove a dead-end product 5-methylthiopentyl (MTA)[35,36].

The RuBisCO carboxylation and oxygenation process starts with the carboxylation of a lysine of the RuBisCO N-terminal domain by a non-substrate CO_2 (carbamylation) and then a Mg^{2+} binds to and stabilizes it[37]. Afterwards, RuBP binds to the active site and is enolized to enediol, followed by the topology structure change of loop 6 and the flexible tail of the C-terminal domain, closing the active site. Now the active site is ready to bind the substrate CO_2 or O_2. During the multi-step catalytic process, RuBisCO is inhibited by kinds of sugar phosphate. It can be inhibited by its own substrate RuBP, which binds to the uncarbamylated RuBisCO, changes the structure

of the activate site and prevents the attack of CO_2 and O_2. It can also inhibited by some other inhibitors, derivate from unstable intermediates during the multi-step catalytic processes (self-inhibition). Among these inhibitors, xylulose-1,5-bisphosphate (XuBP) and 2,3-pentodiulose-1,5-bisphosphate (PDBP) are mostly studied. Some organisms have strategies to escape from these self-inhibitions. For example, RuBisCO from cyanobacteria *Synechococcus* PCC 6301 is able to release XuBP and PDBP fast and avoid the inhibition, while RuBisCO from red algae *Galdieria sulfuraria* has a high CO_2/O_2 specificity, produces less inhibitors thus maintains the enzyme activity[38]. However, in plants, the former two mechanisms do not exist and RuBisCO activity can be inhibited, which is called "fallover". Another inhibitor is 2-carboxy-D-arabinitol-1-phosphate (CA1P), the nighttime inhibitor, which is formed in chloroplasts of plants under low light irradiance or in darkness. Once formed, it binds to the substrate binding site of carbamylated RuBisCO, hindering the anchoring of substrates.

To release the inhibitors and reactivate RuBisCO, an "ATPase associated with various cellular activities" (AAA+) protein, RuBiCO activase (Rca) is required. Rca acts in hexamer form, remodels RuBisCO and releases the inhibitors at the expense of ATP. In some plants, like *Arabidopsis* and spinach, there are two isoforms of Rca, with the α isoform having a longer C-terminus than the β isoform. The longer Rca has the redox regulation target, cysteine residues, which is reduced by f-TRX, activating Rca[39]. The mechanisms of Rca reactivating RuBisCO are not fully understood, especially for eukaryotic Rca. However, there is some understanding on prokaryotic Rca. For example, in the presence of ATP and RuBP, the *Rhodobacter sphaeroides* Rca docks RuBisCO on the conserved top surface of Rca, pulls the C-terminus tail of the RuBisCO large subunit and opens the closed active sites to activate RuBisCO[40]. In *Acidithiobacillus ferrooxidans* and *Halothiobacillus neapolitanus*, Rca requires a RuBisCO adaptor protein CbbO to stimulate the ATPase activity of Rca before Rca is available to activate the RuBisCO[41,42].

Aldolase

Aldolase (FBA, EC 4.1.2.13) catalyzes the reversible aldol condensation of dihydroxyacetone phosphate (DHAP) and GAP to fructose-1,6-bisphosphate (FBP), which is FBP aldolation function. It can also catalyze DHAP and erythrose-4-phosphate (E4P) into SBP, which is SBP aldolation function. FBP aldolation function exists in the CBB cycle, glycolysis and gluconeogenesis, while SBP aldolation function is restricted for the CBB cycle. FBA is cataloged into two classes (class I and class II) based on the catalytic mechanisms and distributions in biosphere. The class I FBA exists mainly in eukaryotic organisms, especially in animals and higher plants. It has also been identified in some algae, bacteria and Archaea. The class II FBA main-

ly presents in prokaryotic organisms and in some fungi. The distribution may have some relations with the different catalytic mechanisms of the two FBAs. The class I FBA utilizes a Schiff base reaction mechanism[43], while the class II FBA uses divalent metal ions. The two classes share no homolog of their DNA sequences, which implies separate evolution paths.

In the model cyanobacterium *Synechocystis* PCC 6803, both class I and class II FBAs have been detected, while 90% of FBA activity is from class II FBA. It was predicted that only the class II FBA can catalyze the reactions in the CBB cycle while the deletion of the class I FBA had no obvious effects on the cell growth[44]. In higher plants, FBAs purified from the chloroplast and cytosol show different catalytic activities on FBP and SBP. The chloroplastic FBA has higher SBP to FBP activity than the cytosolic FBA.

FBP/SBPase

The following steps after FBA of the CBB cycle are two irreversible reactions (Fig. 2), dephosphorylating FBP into fructose-6-phosphate (F6P) by fructose-1,6 bisphosphatase (FBPase, EC 3.1.3.12) and dephosphorylating SBP into S7P by sedoheptulose-1,7-bisphosphatase (SBPase, EC 3.1.3.37) in plants.

In eukaryotic organisms, chloroplastic FBPase and cytosolic FBPase coexist, which are homologous. However, compared to the cytosolic FBPase, the chloroplastic FBPase contains 20-30 extra amino acids (loop 170), three cysteines included, which are the TRX regulation target[45]. Another form of chloroplastic FBPase that is not TRX regulated also exists, which emerged later than the TRX regulated FBPase[46]. This form of FBPase has so far only been found in land plants. Unlike FBPase, SBPase is restricted to chloroplasts, which contains CXXXXC motif on the N-terminus. The two cysteines are the targets of redox regulation by ferridoxin/thioredoxin system like the three cysteines in the loop 170 of FBPase.

SBPase and chloroplastic FBPase share high structural homologies, with differences only on the solvent-exposed surface area. FBPase accepts six-carbon substrates, like FBP, and SBPase accepts seven-carbon substrates, like SBP. The evolution of chloroplastic FBPase and SBPase is not the same. Chloroplastic FBPase originated from bacteria and transferred into plant chloroplast by endosymbiosis, while SBPase originated from Archaea[47].

In cyanobacteria, the FBPase and SBPase functions are carried out by a bifunction enzyme FBP/SBPase. In *Synechocystis* PCC 6803, no FBPase other than the bifunctional FBP/SBPase is found and in *Synechococcus elongatus* PCC 7942, the FBPase can be deleted without any obvious phenotype[48]. This means that the FBP/SBPase can catalyze the reaction in gluconeogenesis as cytosolic FBPase does.

Transketolase

Transketolase (TK, EC 2.2.1.1) catalyzes the reversible transfer of a two-carbon glycoaldehyde from keto-sugars to the C-1 aldehyde group of aldo-sugars. In the CBB cycle, it uses the substrates GAP and S7P to form xylulose-5-phosphate (Xu5P) and ribose-5-phosphate (R5P); or GAP and F6P to produce Xu5P and E4P. In the OPP pathway, it catalyzes the reverse reactions. The TK activity requires the cofactor thiamine pyrophosphate (TPP), the active form of vitamin B1 thiamine. Synthesis of thiamine needs GAP and R5P, which are substrates and products of TK in the CBB cycle respectively. Therefore, there are some circuit regulations on TK activity and TPP levels in the cells. E4P, the product of TK in the CBB cycle, is one of the precursors of shikimic acid pathway. The shikimic acid pathway synthesizes aromatic amino acids, which are precursors to phenylpropanoid, one of the secondary metabolites synthesized through phenylpropanoid metabolism pathway. It was observed that decreasing the TK activity until certain levels in tobacco cells not only inhibited photosynthesis, especially under high irradiance condition, but also inhibited the formation of aromatic amino acid and phenylpropanoid[49]. Therefore, TK is an important enzyme in both primary metabolism (the CBB cycle and the OPP pathway) and secondary metabolism (the shikimic acid pathway and phenylpropanoid metabolism pathway). Any change of TK activity may lead to wide effects on the carbon metabolisms in the cells.

The four enzymes introduced above are the potential targets for the CBB cycle engineering to increase the carbon fixation efficiency. The literature reports of overexpressing one or more of the four CBB cycle enzymes discussed above are summarized in Table 1.

Table 1. Literature reports of the four CBB enzymes expressed in various hosts.

Enzyme	Host	Source	Main effects
RuBisCO	*Synechococcus elongatus* PCC 7942	*Allochromatium vinosum*	1.5 to 4 fold increase of RuBisCO activity; 1.6 times higher of total photosynthesis activity[28]
	Synechococcus elongatus PCC 7942	*Synechococcus elongatus* PCC 6301	1.4 fold increase in total RuBisCO activity; Unchanged photosynthetic O_2 production; 2 fold higher in isobutyraldehyde production[50]
	Synechococcus elongatus PCC 7942	*Synechococcus elongatus* 7942	Unchanged oxygen evolution and free fatty acids production[51]
	Synechococcus PCC 7002	*Synechococcus elongatus* PCC 7942	3 fold increase of free fatty acids production[52]
	Tobacco, *Nicotiana tabacum*	*Synechococcus elongatus* PCC 7942	Higher rates of CO2 fixation per unit of enzyme, autotrophic growth only rely on cyanobacterial RuBisCO under 3% CO_2 condition[53]

	Synechococcus elongatus PCC 7942	*Synechococcus* PCC 7002	Positive effects on growth and 2,3-butanediol production using 10g/L glucose in the BG11 medium when cooverexpressed with PRK, OPP enzymes and galactose transporter[54]
	Synechococcus elongatus PCC 7942	Synechococcus elongatus *PCC 7942*	No significant effects on growth and 2,3-butanediol production using 10g/L glucose in the BG11 medium[54]
Chloroplastic FBPase	*Anabaena* PCC 7120	Wheat	1.4 fold higher FBPase activity, increased net photosynthesis (117.2%) and true photosynthesis (122.5%), faster growth and more chlorophyll a under atmospheric conditions (360 μmol mol^{-1} CO_2)[55]
	Chlamydomonas reinhardtii	*Chlamydomonas reinhardtii*	1.4 fold higher FBPase activity, slower photoautotrophic growth with or without elevated CO_2 levels[56]
Form II FBPase	Tobacco, *Nicotiana tabacum cv. Xanthi*	*Synechococcus elongatus* PCC 7942	Transformant line with 2.3 fold higher FBPase activity had higher dry matter under atmospheric condition, photosynthetic activity under saturated light intensity, RuBP level, *in vivo* RuBisCO activation state, and hexose, sucrose and starch concentration in upper and lower leavies[57]
FBP/SBPase	Tobacco	*Synechococcus elongatus* PCC 7942	Increased photosynthetic CO2 fixation, photosynthesis, growth, RuBP and GAP concentration, initial RuBisCO activity (probably due to higher RuBP concentration) under atmospheric condition[58]
	Euglena gracilis	*Synechococcus elongatus* PCC 7942	Larger cell volume under 100 μmol photons m^{-2} s^{-1} and 0.04 % CO_2, enhanced biomass and photosynthetic activity under high light and high CO_2, increased wax esters production on anaerobiosis[59]
	Soybean, *Glycine max*	Cyanobacteria	Increased carbon assimilation (4-14%), RuBP regeneration capacity (4-8%), and maximum carboxylation rate of RuBisCO (5-8%); maintained seed yield under elevated CO_2 (600ppm) and higher temperature[60]
SBPase	Tobacco, *Nicotiana tabacum*	*Arabidopsis thaliana*	Higher photosynthetic capacity, RuBP regeneration capacity, sucrose and starch accumulation, leaf area at the 4-5 leaf stage, and carbon fixation (6-12%)[61]
	Tobacco, *Nicotiana tabacum cv. Xanthi*	*Chlamydomonas*	Increased SBPase activity (1.6 or 4.3 fold), dry matter, photosynthetic CO_2 fixation, growth rate, RuBP contents and RuBisCO activation state[57]

	Rice, *Oryza sativa L.*	Rice, *Oryza sativa L.*	Increased CO_2 assimilation under 30°C and maintained CO_2 assimilation above 30°C[62]
	Tobacco, *Nicotiana tabacum*	*Arabidopsis thaliana*	Enhanced carbon assimilation and RuBP regeneration capacity under elevated CO_2 condition (585ppm)[63]
	Arabidopsis thaliana	*Arabidopsis thaliana*	Increased SBPase activity, leaf area, and photosynthesis carbon fixation rate[64]
FBA	Tobacco, *Nicotiana tabacum*	*Arabidopsis thaliana*	Enhanced growth, increased biomass especially under high CO_2 concentration[65]
	Arabidopsis thaliana	*Arabidopsis thaliana*	Increased accumulation of FBA and FBA activity, photosynthetic CO_2 assimilation rate and more seeds and aerial biomass[66]
	Arabidopsis thaliana	*Arabidopsis thaliana*	Increased FBA activity, PSII efficiency, maximum CO_2 fixation efficiency, and leaf area[64]
	Chlorella vulgaris	*Synechocystis* PCC 6803	FBA activity increased about 1.3 fold; increased CO_2 fixation rate, growth rate and biomass accumulation[67]
TK	Tobacco, *Nicotiana tabacum*	*Arabidopsis thaliana*	Increased TK activity, decreased thiamine levels and leaf area[68]
RuBisCO (the small subunit) and TK	Rice, *Oryza sativa*	Rice, *Oryza sativa*	Increased RuBisCO and TK amount, similar CO_2 assimilation rate as wild type[69]

Alternative carbon fixation pathways

Not only the CBB cycle, but also the alternative natural and synthetic carbon fixation pathways are intensively studied. The focus of these studies is the carbon fixation efficiency, which is mainly estimated by pathway kinetics and ATP requirements. The enzymes responsible for carbon fixation in these pathways play important roles on determining the ATP efficiency. In addition to the CBB pathway, the reductive acetyl-CoA pathway (the Wood-Ljungdahl pathway)[70], the reductive TCA (rTCA) cycle[71], the 3-hydroxypropionate (3-HP, the Fuchs-Holo) bicycle[72], the 4-hydroxybutyrate cycles (3-hydroxypropionate/4-hydroxybutyrate, 3-HP/4-HB cycle[73], and dicarboxylate-4-hydroxybutrrate, DC/4-HB cycle[74]) are established naturally existing carbon fixation pathways[75].

The reductive acetyl-CoA pathway is different from the other pathways, including the CBB cycle, in respect to the carbon fixation reactions. In the reductive acetyl-CoA pathway, five sixth of the carbon is assimilated by formate dehydrogenase and CO dehydrogenase/acetyl-CoA synthase. This means that carbon assimilation in this pathway is more reduction dependent

other than carboxylation dependent, while the carbon assimilation of the other five pathways, including the CBB cycle, are purely carboxylation dependent. This makes the reductive acetyl-CoA pathway most ATP efficient and is predicted to have higher biomass yield[76]. However, the carbon fixation product, acetyl-CoA, of the reductive acetyl-CoA cycle needs to be converted into other central carbon metabolism intermediates, like pyruvate and phosphoenolpyruvate, to support cells growth.

The rTCA cycle uses three enzymes, isocitrate dehydrogenase, α-ketoglutarate:ferredoxin oxidoreductase, and pyruvate:ferredoxin oxidoreductase to carboxylate CO_2. The CO_2 assimilation by these three enzymes is reductive reactions, using NADPH (the first one) or ferredoxin (the latter two) as cofactors. The three reactions do not consume ATP. This makes the rTCA cycle more ATP efficient than the CBB cycle. Unfortunately, the latter two enzymes, which use ferredoxin as cofactor, are oxygen sensitive. This restricts the usage of these enzymes to anaerobic conditions. Besides, the rTCA cycle also assimilates one molecule of HCO_3^- by PEPc. The carbon fixation product of the rTCA cycle is also acetyl-CoA, like the reductive acetyl-CoA pathway. Therefore, an acetyl-CoA assimilation pathway is needed.

The 3-HP bicycle consists of two cycles. One is glyoxylate synthesis cycle starting from acetyl-CoA. During this process, bifunctional acetyl-CoA/propionyl-CoA carboxylase assimilates HCO_3^-. This cycle regenerate acetyl-CoA and synthesize glyoxylate. The second one is pyruvate synthesis cycle starting from glyoxylate and propionyl-CoA, releasing pyruvate and regenerating acetyl-CoA. The ATP cost of the 3-HP bicycle is high. However, the advantage of the 3-HP pathway over the rTCA cycle is oxygen insensitivity and over the CBB cycle is the absence of competition photorespiration reaction.

The two 4-HP cycles, 3-HP/4-HB cycle and DC/4-HB cycle, assimilate two molecules of inorganic carbon into acetyl-CoA separately. Then the acetyl-CoA is converted into central carbon metabolisms through different pathways. 3-HP/4-HB cycle uses acetyl-CoA/propionyl-CoA carboxylase and requires 3mol ATP to fix one molecule of CO_2, while DC/4-HB employs pyruvate:ferredoxin oxidoreductase and PEPc and requires 1.6mol ATP to fix one molecule of CO_2[74]. This low ATP requirement benefits from the reduction reaction catalyzed by pyruvate:ferredoxin oxidoreductase, and no ATP is consumed in this reaction. However, this also makes the DC/4-HB cycle oxygen sensitive.

Conclusively, the ATP efficient pathways, like rTCA cycle and DC/4-HB cycle usually possess carbon assimilation enzymes that catalyze the reductive reactions, like pyruvate:ferredoxin oxidoreductase. However, these enzymes are oxygen sensitive and require strict growth conditions of the rTCA cycle or DC/4-HB cycle possessing organisms. This makes it challenging to

transplant these cycles into oxygen insensitive organisms, like cyanobacteria or *E. coli*.

Recently, another potential CO_2 assimilation pathway was indicated in a dissimilatory phosphite oxidation (DPO) bacterium *Candidatus phosphitivorax*[77]. It is suggested that phosphite is oxidized, providing NADPH to reduce CO_2 into formate by a NADP-dependent formate dehydrogenase. Afterwards, the formate is converted into pyruvate through the reductive glycine pathway[78]. Since phosphite oxidation to phosphate is the most efficient electron providing process, it suggests that this process may drive cell growth under energy limit conditions. The carbon fixation during this process is mainly reduction dependent, which means it is ATP efficient. If an oxygen insensitive formate dehydrogenase was applied, the reductive glycine pathway will be oxygen tolerant. This makes it promising to be transplanted into aerobic organism.

Instead of understanding, transplanting and engineering the native carbon fixation pathways, assembling an artificial carbon fixation pathway is another attractive strategy to improve carbon fixation efficiency. Bar-Even et al. examined 5000 native existing enzymes for alternative synthetic carbon fixation pathways[79]. Focusing on the pathway kinetics, thermodynamic feasibility, oxygen insensitive, and high energy efficiency (the amount of NADPH equivalents and ATP equivalents cost to produce one molecule of product), they modeled a pathway using PEPc to fix CO_2 and generating glyoxylate out of the cycle, which was named malonyl-CoA-oxaloacetate-glyoxylate (MOG) pathway. The starting reactions of this pathway are overlapped with the C4 carbon fixation pathway in the mesophyll cell, but the MOG pathway does not include the reactions in the bundle-sheath cells, meaning it avoids the usage of RuBisCO. Modulation showed that this pathway is 2 to 3 folder faster at fixing carbon than the CBB cycle[79]. Although the whole pathway has not been tested experimentally, it has been reported that overexpressing PEPc in *Synechocystis* PCC 6803 enhanced the cell growth under low light conditions[80].

There is another synthetic carbon fixation pathway, crotonyl–CoA/ethylmalonyl-CoA/hydroxybutyryl-CoA (CETCH) cycle, that has been examined *in vitro*[81]. The CETCH cycle uses enoyl-CoA carboxylases/reductases, which does not exist in autotrophic CO_2 fixation organisms, to carboxylate CO_2. After enzyme modification or replacement, a well functional CETCH 5.4 is generated and actives *in vitro*. This cycle includes 13 enzymes in the carbon fixation cycle and 5 enzymes for auxiliary proofreading (converting glyoxylate into malate) and cofactor regeneration. Glyoxylate was the output of the carbon fixation cycle in CETCH 5.4, in which two CO_2 were fixed into glyoxylate on the expense of two ATP and three NADPH, more energy-efficient than the CBB cycle[81].

Introducing synthetic pathways into the living organisms may be challenging because of the interference between the artificial metabolism and the

background native metabolisms of the host. However, testing the function of the synthetic pathways *in vitro* with considering and mimicking the *in vivo* conditions is a big step towards establishing complicated synthetic pathways into living organisms.

Protein fusion domains (tags)

Recombinant technology is widely used in protein expression and purification[82]. This technology is adding an extra sequence, which can be as short as several amino acids and as long as a whole peptide, on the N-terminus or the C-terminus of the target protein. When deciding the position of the tag, it is reasonable to check the structure of the target protein and add the tag on the "free" end, which ensures the tag not be buried into the tertiary structure. The tag can be directly fused to the target protein without any spacer between, mostly for a small tag since it is small enough to may have no effects on the target protein. In many cases, there will be a linker between the tag and the target protein to make sure that the addition of the tag will not affect the structure and/or activity of the target protein. If removing the tag is required after protein expression and/or purification, a protease specific-site will be designed, which could also act as a linker.

The purposes of adding a tag on the target protein vary, including improving protein expressing or solubility, detecting the localization of target protein, getting protein expression image, quantifying protein, purifying protein, and some other purposes[83,84]. Protein tag can be divided into two groups, affinity tag and solubility tag, which could be easily understood by the group names[85]. For recombinant protein with affinity tag, the corresponding affinity matrix is used to purify the protein. Frequently used affinity tag includes His-tag (six His), attaching to immobilized metal ions, Ni, Co, Cu, Zn, FLAG-tag (eight amino acids, DYKDDDDK), attaching to anti-FLAG mAB, and Strep-II-tag (eight amino acids, WSHPQFEK), attaching to Strep-Tactin. The basis of the solubility tag is a highly translated native gene tagging on the N-terminus of the heterologous gene, like the maltose-binding protein (MBP) gene. It does not necessarily mean that one tag is restricted within one group. Some tags, like the glutathione-S-transferase (GST) tag and MBP, can be used as affinity tags as well as improving protein solubility[86].

Many factors need to be considered when choosing a tag for recombinant protein expression, the size of the tag and target protein, purification cost, potential effect(s) on protein folding and stability, effect(s) on protein expressing, and so on. For example, if the affinity tag was much larger than the target protein, a much higher amount of recombinant protein need to be purified to make sure that the target protein can reach certain amount. In this case, a smaller tag may be a better option. Besides, the cost of the affinity

matrix, the compatibility between purification methods and the features of the target protein should also be taken into consideration. The position of a tag might have effects on gene expression or/and protein structure. A Tag on the N terminus of target protein may have effects on the 5' untranslated region (5'UTR) of the gene, resulting in unpredictable translation efficiency[87]. On another hand, a solubility tag usually enhances the protein expression level, which may not be suitable to use when low expression is required. This problem could be mitigated by using tandem tags[88].

In many cases, the tag does not change the structure and biological activity of the target protein, especially the small tag[89]. Therefore, it is not necessary to remove the tag after protein expression and/or purification. However, it may be still optimal to remove them. It has been reported that a small tag, FLAG on the C terminus of glutamate dehydrogenase (GDH) decreased its sensitivity to adenosine diphosphate (ADP) activation[90]. In some other cases, the tag may have dramatic effects on the protein structure and/or activity, especially the large tag like GST or MBP[86]. Thus the tag has to be removed after protein expression and/or purification. Under these circumstances, a specific amino acid sequence, cleavage site, is designed between the tag and the target protein. The sequences of the cleavage site are rarely found in the target protein. Therefore when the site-specific protease supplied, it does not digest the target protein but allows the removal of the tag. In reality, the protease cleavage is usually challenged by unspecific and incomplete cleavage. As contrast, chemical cleavage could be more efficient. However, the conditions for chemical cleavage are harsh, which would result in the denaturation of the protein, which would be a big problem if reconstitution of the protein is difficult or impossible[91]. No matter which method is used to remove the tag, another affinity chromatography is usually required to separate the tag, protease or chemical reagents from the target protein.

Cyanobacterial cell factories

As discussed above, more and more life essentials are required as society develops and world population increases. Besides, the stock of fossil fuels is running low and undesired byproducts, like dust and sulfur compounds, are produced during the treatment of fossil fuels. Renewable and clean sources are highly required.

One way to get renewable and clean sources is to supply plant biomass to *E. coli*, yeast or other well understood organisms to ferment for desired compound. However, due to the multiple steps in this process, from energy absorption by plants to fermentation by heterotrophic organisms, the energy efficiency (solar energy to product) is very low, for example 0.2% in ethanol production from sugarcane[92]. Besides, *E. coli* and yeast fermentation has limitations on the available sugar forms. The most abundant carbohydrate,

lignocellulose from plant materials, needs to be broken down into smaller molecular before applied to the organisms, which requires expensive steps using enzymes, high temperature, or/and high pressure[93]. Additionally, using plants in the form of crops as fermentation sugar sources leads to less arable land for food production, which will make food more expensive.

Another way is to extract renewable and clean sources directly from autotrophic organisms, like cyanobacteria. Using autotrophic organisms as cell factories or cell catalysts has many advantages over the traditional fermentation technologies, like the cheap and abundant energy (sun light) and carbon (CO_2) sources, and higher energy efficiency (1.5% in the oil production from microalgae)[94]. Besides, cyanobacteria are the only prokaryotic oxygenic organisms, which means it is relatively easier to be metabolically engineered compared to any eukaryotic oxygenic organisms, like microalgae. The ideal cyanobacteria factory or cyanobacteria catalyst will maintain the cell population as well as distribute the remaining energy and carbons to the designed product. It will be even better if they can excrete the products out of the cells since this will minimize the effects from the products and increase the yield of the products[95,96]. To excrete the product is especially important when something toxic is produced or when it has negative effects on the native metabolism.

Fortunately, a lot of genetic tools are available to engineer cyanobacteria, such as synthetic biology tools and computational modeling[97–100]. The newly developed genome editing method, CRISPR/Cas9, has already been applied in cyanobacteria[101,102], which makes it easier to handle multiple genes and stubborn genes that are difficult to be modified using traditional genetic tools. Flux balance analysis and kinetic modeling, which is more difficult to apply in cyanobacteria, are two representative computational models and already used in cyanobacteria[103,104]. Both of them are valuable at predicting carbon distribution and guiding genetic engineering[105].

Cyanobacteria are able to produce many different compounds[106]. The synthetic pathways of most of the compounds start from an intermediate of the central carbon metabolism. Some are from pyruvate, like ethanol, butanol, and lactate. Some are from Acetyl-CoA, like alkanes, and fatty acids. Some are from the TCA cycle, like ethylene. Some products' synthetic pathways start from two central intermediates, like the methylerythritol 4-phosphate (MEP) pathway that starts from GAP and pyruvate. This pathway synthesizes e.g. squalene, and isoprene. Hydrogen (H_2) is different since it is not a carbon-based compound. It is produced through H^+ receiving electrons from the light reaction through NADPH or ferredoxin. Besides the advantages of producing a diversity of chemicals, the cyanobacteria factory concept is an optimal option especially for products that are originally synthesized in plants[107].

Despite all the advantages of cyanobacteria as cell factories over the traditional fermentation method, low yield is one of the main obstacles to com-

mercialize cyanobacterial products since low yield means that the cost per unit is too high. There are different strategies to increase the desired compounds production in cyanobacteria, summarized in the chapter "Engineering Cyanobacteria for Biofuel Production", which includes optimizing light harvesting capacity, increasing carbon assimilation (further investigated in this thesis), and redirecting the carbon flux (paper V). In addition, the status on cyanobacterial biofuels and hydrogen (H_2) studies are also included.

Aim

The object of this work is the Calvin-Benson-Bassham (CBB) cycle in the model cyanobacterium *Synechocystis* PCC 6803. General questions to be answered include

1. How to engineer cyanobacteria to fix more carbon and grow faster (paper I, II and V);

2. Effects on photosynthesis, cell growth and biomass accumulation by overexpressing the CBB cycle control enzymes (paper I, II);

3. Possibility to increase the desired compound production by using cells with engineered CBB cycle (paper III, IV).

Results and Discussion

Four enzymes of the Calvin-Benson-Bassham (CBB) cycle, RuBisCO, FBP/SBPase, FBA and TK, were selected as targets to study the effects on photosynthesis, growth, biomass accumulation and compound formation (exampled as ethanol) by overexpressing them individually in *Synechocystis* PCC 6803 (hereafter *Synechocystis*). Engineered *Synechocystis* strains are all listed in Table 2.

Table 2. Engineered *Synechocystis* strains used in this thesis. Enzyme names refer the abbreviation list.

Position	Studied Enzyme(s)	Gene(s)	*Synechocystis* Strains	Paper
Shuttle vector, pPMQAK1[97]			control	I, IV,
			WT+Km^r-vector	II
			empty	III
	Synechocystis RuBisCO	*slr0009-slr0011-slr0012*	rbc	I, II
	Synechocystis CcmM	*sll1031*	ccmM	I
	Synechocystis FBP/SBPase	*slr2094*	fbpI	I
	Synechocystis FBA, class I	*slr0943*	fbaI	I
	Synechocystis FBA, class II	*sll0018*	fbaA	I
	Synechocystis TK	*sll1070*	tktA	I
	Synechococcus enlongatus PCC 7942 FBP/SBPase	*Synpcc7942_0505*	79glpX	I
	Synechococcus PCC 7002 FBP/SBPase	*SYNPCC7002_A1301*	70glpX	I
	Synechocystis RuBisCO with FLAG tag on large subunit N terminus	FLAG- *slr0009-slr0011-slr0012*	FL50	II
	Synechocystis RuBisCO with FLAG tag on large subunit C terminus	*slr0009*-FLAG-*slr0011-slr0012*	FL50C	II
	Synechocystis RuBisCO with FLAG tag on small subunit C terminus	*slr0009-slr0011-slr0012*-FLAG	FL52	II
	Synechocystis RuBisCO with strep tag II on large subunit N terminus	strep tag II-*slr0009-slr0011-slr0012*	FL50strep	II

	Synechocystis RuBisCO with strep tag II on small subunit C terminus	*slr0009-slr0011-slr0012*-strep tag II	FL52strep	II
Genome loci *slr0168*			WT+Km^r-genome	II
	Synechocystis RuBisCO with FLAG tag on the large subunit N terminus	FLAG- *slr0009-slr0011-slr0012*	FL50G	II
	Synechocystis RuBisCO with FLAG tag on the small subunit C terminus	*slr0009-slr0011-slr0012*-FLAG	FL52G	II
Upstream of genome loci *slr0009*		A kanamycin cassette with P*psbA2* and FLAG tag in order inserted into the upstream of *slr0009*, after ATG of *slr0009*	FL75	II
Downstrem of genome loci *slr0012*		FLAG tag and a kanamycin cassette in order inserted into downstream of *slr0012*, in front of TAA of *slr0012*	FL76	II
Shuttle vector, pPMQAK1[97]	EFYP	*efyp*	PnrsB_EYFP	III
	Zymomonas mobilis PDC and *Synechocystis* ADH	*pdc, slr1192*	PnrsB_EtOH/EtOH	III/IV
	Synechocystis RuBisCO with FLAG tag on the small subunit C terminus, *Zymomonas mobilis* PDC and *Synechocystis* ADH	*pdc, slr1192*, FLAG- *slr0009-slr0011-slr0012*	EtOH-rbcSC	IV
	Synechococcus PCC 7002 FBP/SBPase, *Zymomonas mobilis* PDC and *Synechocystis* ADH	*pdc, slr1192, SYNPCC7002_A1301*	EtOH-70glpX	IV
	Synechocystis TK, *Zymomonas mobilis* PDC and *Synechocystis* ADH	*pdc, slr1192, sll1070*	EtOH-tktA	IV
	Synechocystis FBA class II, *Zymomonas mobilis* PDC and *Synechocystis* ADH	*pdc, slr1192, sll0018*	EtOH-fbaA	IV

Effects of overexpressing selected CBB cycle enzymes individually in *Synechocystis* (paper I)

Four enzymes, RuBisCO, FBP/SBPase, FBA and TK, were selected as potential targets to increase carbon fixation in *Synechocystis*. To overexpress RuBisCO, both the RuBisCO gene (*slr0009-slr0012-slr0012*) and the carboxysome protein CcmM gene (*sll1031*) were amplified from *Synechocystis* genome and expressed individually in *Synechocystis*. This is based on the knowledge that RuBisCO is located in the carboxysome in cyanobacteria and the carboxysome protein CcmM is essential to pack RuBisCO (small version of CcmM), and bind RuBisCO to the shell and carbonic anhydrase (full version of CcmM[13]). To overexpress FBP/SBPase, three genes from three different cyanobacterial strains were used, *slr2094* from *Synechocystis*, *Synpcc7942_0505* from *Synechococcus elongatus* PCC 7942 and *SYNPCC7002_A1301* from *Synechococcus* PCC 7002. Therefore, both homogenous and heterologous FBP/SBPase expressions and effects were studied. To overexpress FBA, the two FBA genes from *Synechocystis*, *slr0943* encoding class I FBA and *sll0018* encoding class II FBA[44], were used. The two FBAs have different catalytic mechanisms, which makes it interesting to determine which version works better in cyanobacteria. To overexpress TK, the gene *sll1070* from *Synechocystis* was used. The genes used and the corresponding engineered strains are listed in Table 2. All the genes were driven by *Synechocystis* native P*psbA2* and expressed on the RSF1010 based shuttle vector pPMQAK1[97]. The growth of wild type strain and the strain containing the empty shuttle vector was different under 100μmol photons m^{-2} s^{-1} light intensity, one of the light intensities used in the following experiments. Therefore, the strain containing empty vector (control strain in Table 2) was used as the reference strain instead of the wild type strain.

The engineered *Synechocystis* strains (Table 2, paper I) were cultivated under 15μmol photons m^{-2} s^{-1} and 100μmol photons m^{-2} s^{-1} light intensities in 100ml Erlenmeyer flasks, shaking. Under both light conditions, the RuBisCO level was not increased in strain rbc. Interestingly, the RuBisCO level increased in strain ccmM under both conditions, even though it was difficult to tell if the CcmM level changed (Figs. 3A and 3C). The carboxysome level in the ccmM strain was not determined. In cyanobacteria, both the long and short CcmMs are essential for RuBisCO to be localized in the carboxysome[13]. Thus the positive effects on RuBisCO level by *sll1031* engineering detected here may be due to the potential positive effects of CcmM on localizing RuBisCO into the carboxysome.

To further investigate the possible reasons to the non-increased RuBisCO level in the rbc strain, semi-quantitative reverse transcription PCR (RT-PCR) was conducted. The RuBisCO gene on the shuttle vector was transcribed successfully without any transcription decrease of the original copy on the genome (Fig. 4). In another words, the mRNA level of the RuBisCO gene

was higher in the rbc strain than in the control strain under both 15μmol photons m^{-2} s^{-1} and 100μmol photons m^{-2} s^{-1} light conditions. Therefore, post-transcriptional regulations, like initiation of translation, modifications of protein, and protein stability may play roles in controlling the RuBisCO level and be responsible for the non-increased RuBisCO in the rbc strain. Considering the RuBisCO level increased in the ccmM strain, RuBisCO stability may be a highly possible explanation.

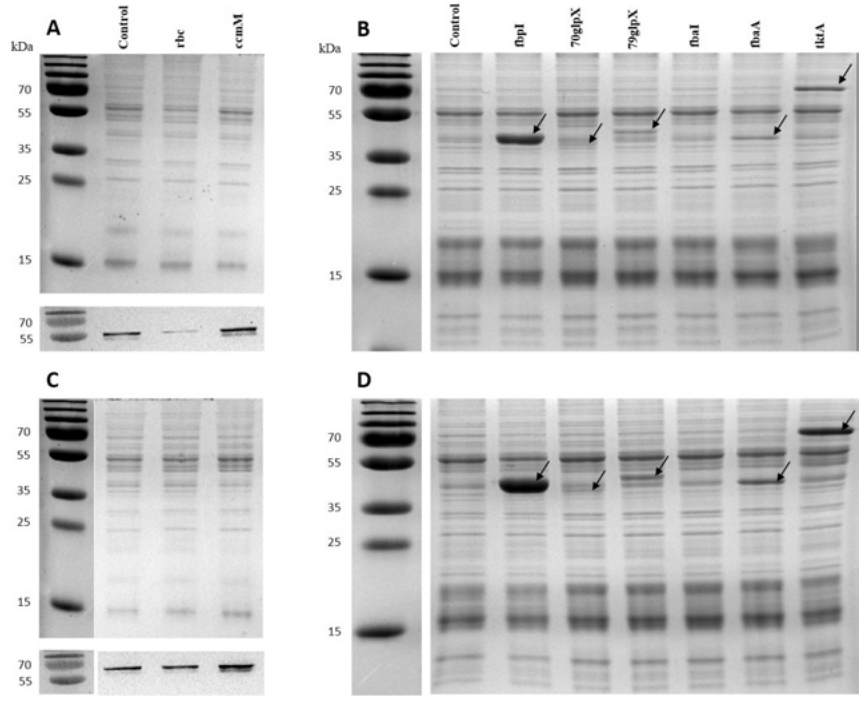

Figure 3. SDS-PAGE (upper panel of A, B, upper panel of C, and D) and Western immunoblot using antibodies against RuBisCO large subunit (lower panel of A and lower panel of C) of *Synechocystis* engineered strains. A and B are samples cultivated under 15μmol photons m^{-2} s^{-1}. C and D are samples cultivated under 100μmol photons m^{-2} s^{-1}. The arrows indicate the overexpressed proteins detected on the SDS-PAGE. For strain details, see Table 2. Figure is modified from paper I.

For strains fbpI, 70glpX, 79glpX, fbaA and tktA, it was easy to observe the overexpression of the corresponding enzymes (indicated by arrows, Figs. 3B and 3D) on the SDS-PAGE gels, based on the predicted protein molecular weights. For strain fbaI, no obvious overexpression was observed on the SDS-PAGE gels under both light conditions (Figs. 3B and 3D).

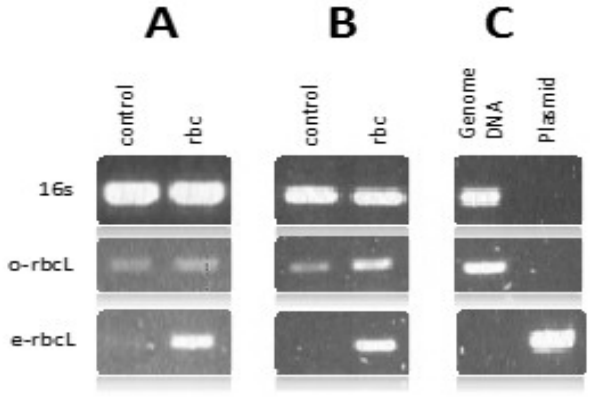

Figure 4. RT-PCR of the *Synechocystis* control and rbc strains. o-rbcL indicates the transcription level of the original RuBisCO gene on the chromosome. e-rbcL indicates the transcription level of the extra RuBisCO gene on the shuttle vector. A is the samples cultivated under 15μmol photons m^{-2} s^{-1} and B is the samples cultivated under 100μmol photons m^{-2} s^{-1}. C shows controls using genome DNA and the conjugation plasmid as the template. Figure is from paper I.

Growth of the engineered strains was determined by optical density at 750nm wavelength (OD_{750}) and chlorophyll a content. Both the OD_{750} and chlorophyll a content quantification showed that under 15μmol photons m^{-2} s^{-1} light intensity, the engineered strains did not grow faster than the control strain (even slower, Figs. 5A and 5B). In contrast, under 100μmol photons m^{-2} s^{-1}, strains ccmM, fbpI, 70glpX, 79glpX, fbaI, and fbaA grew faster than the control strain, indicated by both OD_{750} and chlorophyll a content (Figs. 5C and 5D). The rbc and tktA strains grew slower than the control strain, indicated by both OD_{750} and chlorophyll a content (Figs. 5C and 5D). Among the faster growing strains, only fbaI strain did not show overexpression on the SDS-PAGE gels. However, it still showed similar phenotype with the fbaA strain. More experiments are required to elucidate the similar phenotype. The different catalytic mechanisms of the two FBAs may be one of the reasons. Under low light, growth was inhibited by light inefficiency. The overexpression of the CBB cycle enzymes cannot result in positive effects on growth because the light reaction is restricted. Instead, the overexpressed enzymes consume carbon and nitrogen sources, which may lead to the negative effects on the growth. Under higher light, positive effects on growth were detected in the strains that had increased RuBisCO, FBP/SBPase and FBA protein levels. It is not clear why the rbc strain grew slower since the Western immunoblot showed that the RuBisCO level was unchanged (Fig. 3C). For strain tktA, the negative effects on growth may partially due to the interruption on the thiamine balance, which was observed in tobacco cells with more TK[49].

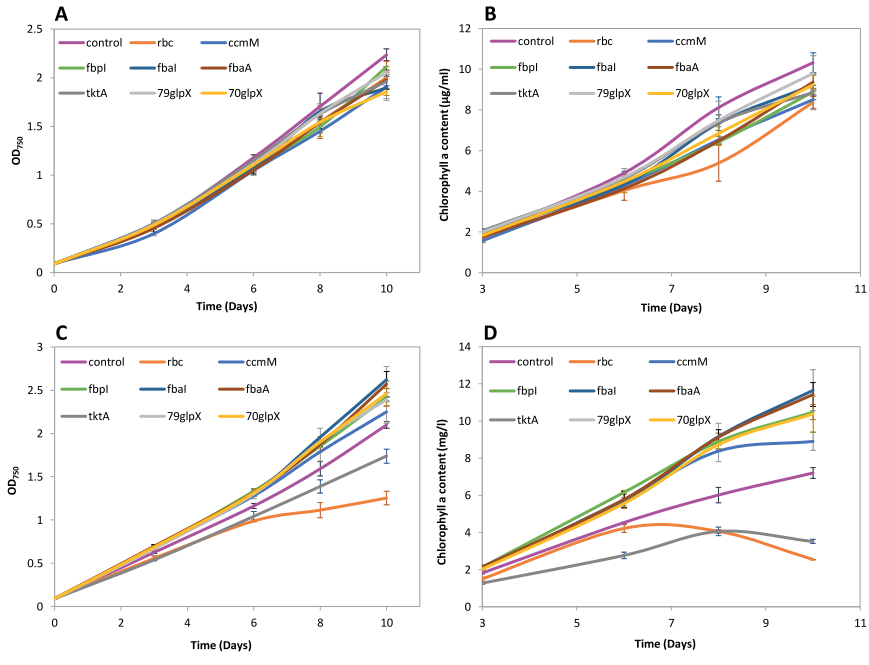

Figure 5. Growth of engineered *Synechocystis* strains indicated by optical density at 750nm wavelength (OD_{750}, A and C) and chlorophyll a content (B and D). Cells were cultivated in flasks without air bubbling or extra carbon supply. A and B show the growth of cells cultivated under 15µmol photons m^{-2} s^{-1}. C and D are growth of cells cultivated under 100µmol photons m^{-2} s^{-1}. Error bars indicate standard deviations of biological triplicates. For strain details, see Table 2.

Net oxygen evolution rate, under saturated light intensity instead of the actual cultivation light, was determined to check the efficiency of photosystem II using cells in exponential phase. For the cells collected from 15µmol photons m^{-2} s^{-1} light intensity, strains ccmM, fbpI, 79glpX, 70glpX, fbaI, fbaA and tktA showed increased net oxygen evolution rate compared to the control stain, by 53%, 66%, 27%, 45%, 59%, 90% and 85%, respectively. The difference between the rbc strain and the control strain was not statistically significant (Fig. 6A). The results indicate that the low light adapted cells still have the ability to split water faster than the control strain but the low cultivation light limits the growth rate. For cells collected under higher light intensity, 100µmol photons m^{-2} s^{-1}, significantly increased net oxygen evolution rate was observed in strains fbpI, 79glpX, 70glpX, fbaI and fbaA, by 41%, 98%, 125%, 52%, and 51% respectively, compared to the control strain. In the ccmM strain, the increase was not statistically significant. The rbc and tktA strains showed decreased net oxygen evolution rate under this light condition (Fig. 6B), which was not surprised since the rbc and tktA strains showed decreased chlorophyll a content under this light intensity (Fig. 5D).

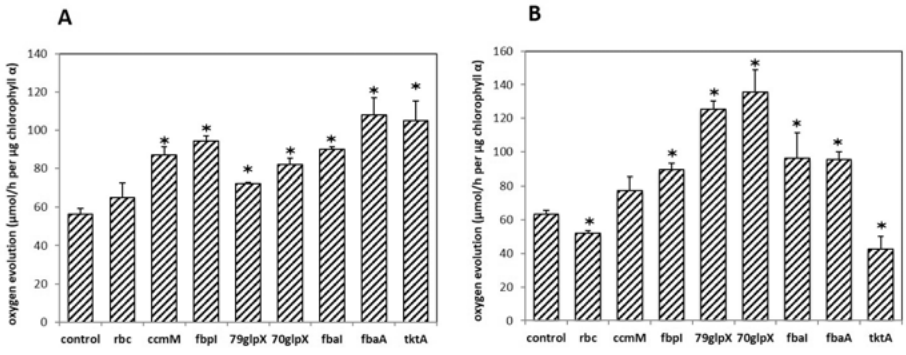

Figure 6. Net oxygen evolution rate under saturated light intensity. A shows samples collected under 15μmol photons m^{-2} s^{-1} light intensity. B shows samples collected under 100μphotons m^{-2} s^{-1}. Error bars are standard deviations of biological triplicates. Asterisks indicate the significant difference ($P<0.05$) between the engineered strains and the control strain according to one-way ANOVA analysis. For strain details, see Table 2. The figure is modified from paper I.

The dry cell weight (DCW) after 10 days cultivation was determined to indicate the amount of carbon fixed into biomass. When cells were cultivated under 15μmol photons m^{-2} s^{-1} light intensity without bubbling air or supplying extra carbon, the tktA strain accumulated more DCW (24% more) than the control strain (Fig. 7A) even though the growth, indicated with OD_{750} and chlorophyll a content, was not faster than the control strain (Figs, 5A and 5B). The other CBB cycle genes overexpressed strains did not accumulate more DCW than the control strain (Fig. 7A), which was consistent with the growth (Figs, 5A and 5B). Under 100μmol photons m^{-2} s^{-1} light intensity condition, the DCW of the tktA strain was 42% higher than the control strain (Fig. 7B), again inconsistent with the growth (Figs. 5C and 5D). The DCW of ccmM, fbpI, 79glpX, 70glpX, fbaI and fbaA strains were 24%, 52%, 26%, 38%, 49% and 50% higher than the control strain respectively (Fig. 7B). The increase of ccmM strain was not statistically significant though. The DCW accumulation of the rbc and the control strains were almost the same (Fig. 7B). Increasing TK level in the *Synechocystis* cells led to increased DCW accumulation under both light conditions used in this study. However, the DCW accumulation and the growth of the tktA strain were inconsistent. The reasons to the inconsistency are not clear. However, it has been reported that overexpressing the TK could increase the soluble sugar in cells or increase the size of the leaves in plants[68,108]. Something similar may happen in the *Synechocystis* strain with higher TK level.

Increasing the protein levels of RuBisCO, FBP/SBPase, FBA and TK in *Synechocystis* individually increased the net oxygen evolution rate (indirect proof of enhance photosynthesis efficiency) and DCW accumulation under 100μmol photons m^{-2} s^{-1} light intensity. Besides, the growth of cells with

increased RuBisCO, FBP/SBPase or FBA levels also increased under this condition.

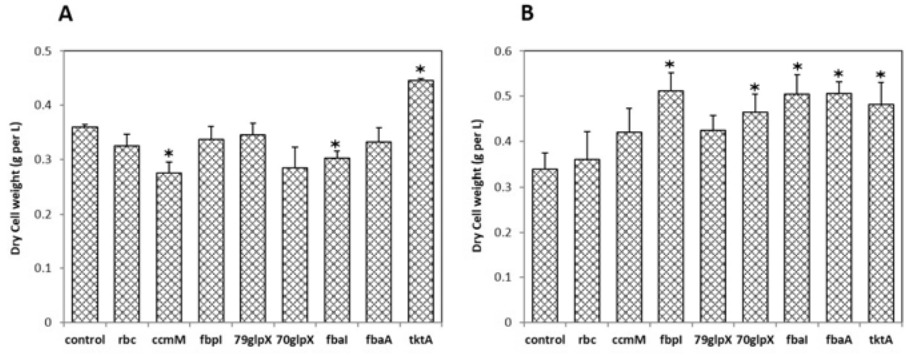

Figure 7. Dry cell weight (DCW) after 10 days of cultivation. The cells were cultivated in flasks without bubbling and extra carbon supply. A shows samples collected under 15μmol photons m^{-2} s^{-1} light intensity. B shows samples collected under 100μphotons m^{-2} s^{-1}. Error bars are standard deviations of biological triplicates. Asterisks indicate the significant difference ($P<0.05$) between the engineered strains and the control strain according to one-way ANOVA analysis. For strain details, see Table 2. The figure is modified from paper I.

Expressing tagged RuBisCO in *Synechocystis* (paper II)

The results showed that introducing another copy of RuBisCO gene (*slr0009-slr0011-slr0012*) on shuttle vector into wild type cells did not increase the RuBisCO level even though the transcription of RuBisCO gene was increased (Fig. 4, paper I). Recombinant protein is a widely used technology for protein expression and purification. This technology is adding a tag on the target protein, which might has positive effects on protein expression, protein solubility, protein folding and so on[84]. Therefore, two tags, FLAG tag and streptavindin-binding tag II (strep tag II), were used for recombinant RuBisCO. Both the FLAG tag and the strep tag II are eight amino acid tags, with the sequence DYKDDDDK and WSHPQFEK, respectively[91].

Two reference strains were developed and used. The strain containing an empty vector (control strain in paper I, WT+Km^r-vector in paper II) was the reference strain for the strains carrying the expression cassette on the shuttle vector pPMQAK1 (strains FL50, FL50C, FL52, FL50strep and FL52strep).

The strain having a kanamycin cassette on the genome loci *slr0168* (WT+Km^r-genome, Table 2, paper II) was the reference strain to the strains having the chromosome RuBisCO gene modified (strains FL75, and FL76) and extra copy of RuBisCO gene on genome loci *slr0168* (strains FL50G and FL52G). For strain details, see Table 2. Strain rbc, containing a second copy of *Synechocystis* RuBisCO gene on the shuttle vector pPMQAK1 (paper I), was also compared in paper II.

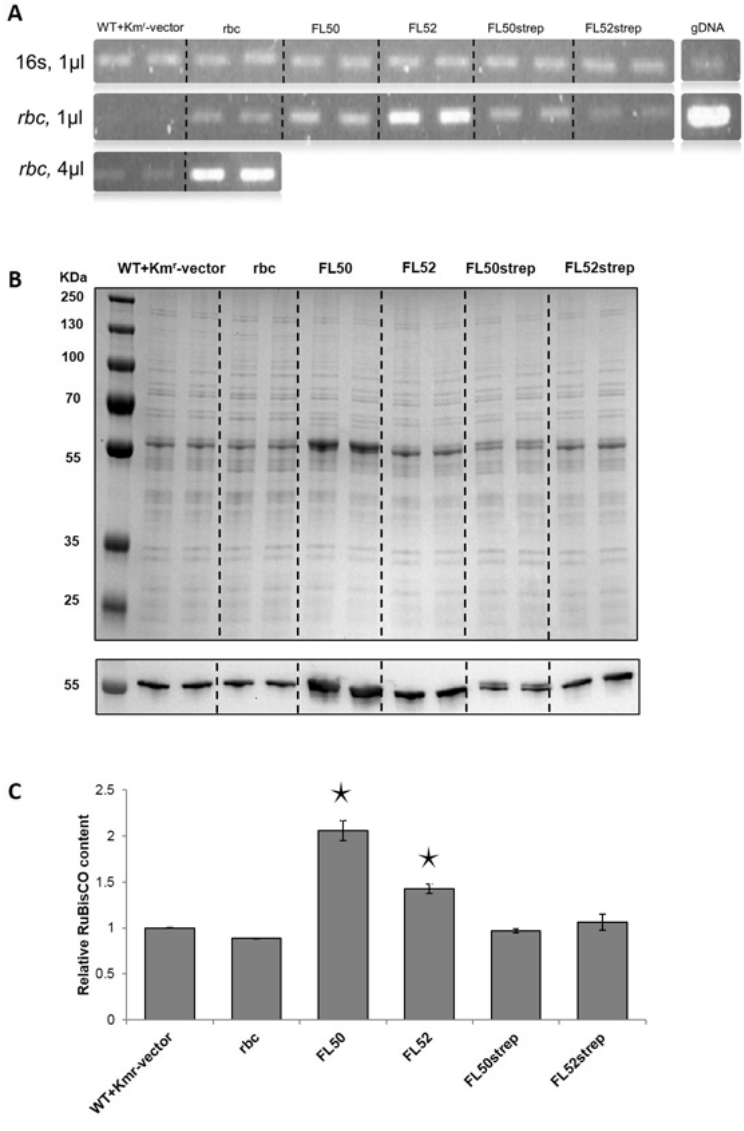

Figure 8. RT-PCR (A, 1µl and 4µl indicate the loading volume), SDS-PAGE (upper panel of B), Western immunoblot using antibodies against RuBisCO large subunit (lower panel of B) and relative RuBisCO content calculated with Quantity one (C). gDNA means the *Synechocystis* genome DNA was used for PCR. The error bars in C are standard deviations from biological duplicates and technical duplicates. Asterisks indicate significant difference ($P<0.05$) between the engineered strains and WT+Km^r-vector strain according to one-way ANOVA analysis. For strain details, see Table 2. The figure is modified from paper II.

The FLAG tag increased the *slr0009* mRNA level no matter it was on the N terminus of the large subunit (in strain FL50) or on the C terminus of the

small subunit (in strain FL52. Fig. 8A) compared to the rbc strain, while the *slr0009* mRNA level of the rbc strain was higher than the WT+Km^r-vector strain (Fig. 4). The FLAG tag also had positive effects on the detected RuBisCO level. In FL50, the RuBisCO level was 2.1 times of that in the WT+Km^r-vector strain, while in FL52, it was 1.4 times (Figs. 8B and 8C). Similar effects were not observed in strain FL50C, where the FLAG tag was on the C terminus of RuBisCO large subunit (Fig. 9). This indicates that the effects of a FLAG tag on RuBisCO expression depend on where the FLAG tag was fused. In FL50strep and FL52strep (Fig. 8), the strep tag II replaced the FLAG tag in FL50 and FL52 accordingly, both mRNA and the protein levels of RuBisCO did not increase compared to that in the rbc strain. This implies that the effects of the tag are sequence specific even though both FLAG and strep tag II are eight amino acids.

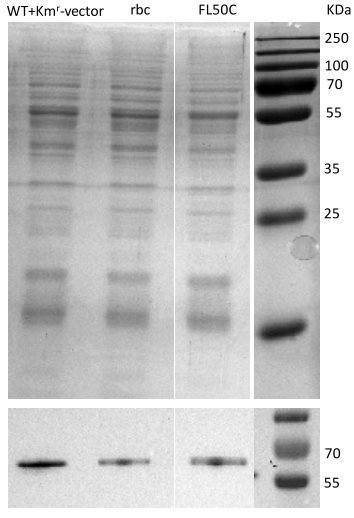

Figure 9. SDS-PAGE (upper panel) and Western immunoblot (lower panel) using antibodies against RuBisCO large subunit of *Synechocystis* strains rbc and FL50C. For strain details, see Table 2. The figure is from paper II.

Till now, it is confirmed that a FLAG tag can enhance the detected RuBisCO level in the cells. Does it have effects on the RuBisCO activity? To address this question, another two strains, FL75 and FL76, were made. In FL75, the genome RuBisCO gene was tagged by FLAG on the N terminus of the large subunit, while in FL76, the genome RuBisCO gene was tagged by FLAG on the C terminus of the small subunit. The full segregation was confirmed with PCR (Fig. 10).

In FL75 and FL76 strains, a kanamycin cassette was inserted into the genome. Therefore, the strain WT+Km^r-genome, which had a kanamycin cassette in the genome loci *slr0168*, was the reference strain. The total RuBisCO activity and specific RuBisCO activity of strains FL50, FL52, FL75 and FL76 were measured and normalized to the corresponding reference

strains. In FL50 and FL52, total RuBisCO activities increased by 52% and 8.6% compared to that in the WT+Km^r-vector strain (Fig. 11A). However, the specific RuBisCO activities were not significantly changed (Fig. 11B). This implies that the FLAG tag does not change the specific RuBisCO activity. The increased RuBisCO activities in strains FL50 and FL52 were because of the increased RuBisCO levels. This was further proved by the unchanged specific RuBisCO activities in strains FL75 and FL76 compared to that in the WT+Km^r-genome strain (Fig. 11B).

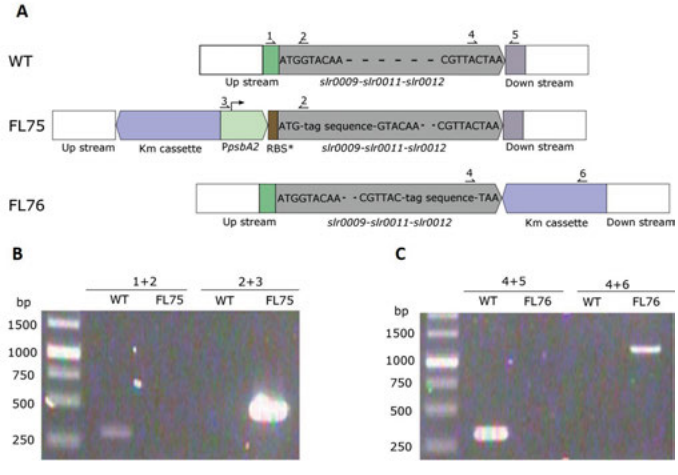

Figure 10. Modified genome RuBisCO gene constructs in strains FL75 and FL76 (A). The full segregation was confirmed with PCR (B and C). WT means *Synechocystis* wild type strain. For strain details, see Table 2. The figure is from paper II.

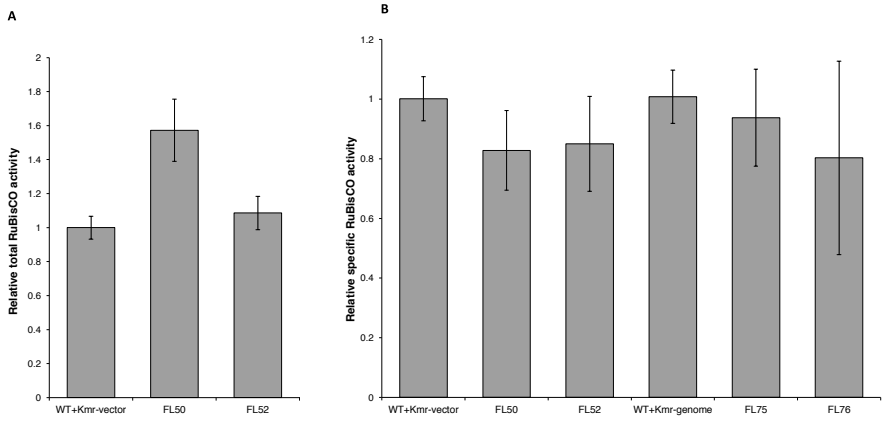

Figure 11. Total RuBisCO activity (A) and specific RuBisCO activity (B) standardized to corresponding reference strains in *Synechocystis* strains FL50, FL52, FL75 and FL76. The error bars are standard deviations from four biological replicates and four technical replicates. For strain details, see Table 2. The figure is modified from paper II.

The RuBisCO gene expression efficiency on shuttle vector and on the genome was also compared. The RuBisCO gene expression cassette on pPMQAK1 in FL50 was amplified and inserted into the genome loci *slr0168*, resulting in the strain FL50G. Similarly, the RuBisCO gene expression cassette on pPMQAK1 in FL52 was inserted into the genome loci *slr0168* of the wild type cells, resulting in strain FL52G (Table 2, paper II). Since the insertion was on the genome and with a kanamycin cassette, strain WT+Km^r-genome was the reference strain. Surprisingly, the RuBisCO levels in FL50G and FL52G did not increase compared to that in the reference strain (Fig. 12). Even though it is reported that in *Synechocystis*, gene expression on shuttle vector pPMQAK1 can be higher than when the same gene is inserted in a neutral site in the genome[109], some degree of increase of the RuBisCO levels was predicated since the FLAG tag showed positive effects on mRNA and RuBisCO levels in strains FL50 and FL52 (Fig. 8). The results indicate that unknown effects on gene expression exist, like the compositional context effects[110]. It is also possible that any difference is too small to be detected with the methods used here.

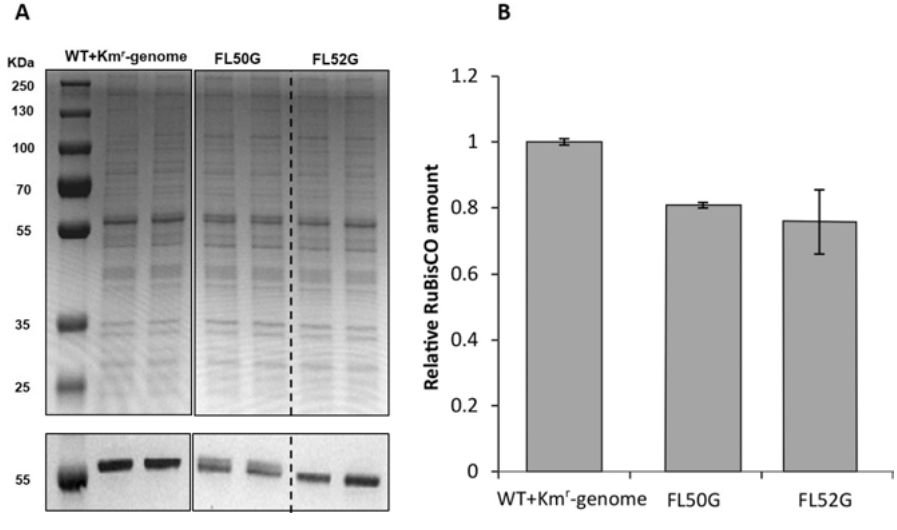

Figure 12. SDS-PAGE (upper panel of A), Western immunoblot using antibodies against RuBisCO large subunit (lower panel of A) and relative RuBisCO amount standardized to the reference strain calculated from the Quantity-one (B) in *Synechocysits* strains FL50G and FL52G. The error bars are the standard deviations from biological duplicates and technical duplicates. For strain details, see Table 2. The figure is modified from paper II.

The FLAG tag, on the N terminus of the large subunit or on the C terminus of the small subunit, had positive effects on mRNA and protein levels of RuBisCO when RuBisCO gene was expressed on the shuttle vector pPMQAK1. However, similar effects were not observed with strep tag II and when RuBisCO gene was expressed on the genome.

Inducible promoter is used for ethanol synthetic pathway (paper III)

Ethanol can be produced in cyanobacteria from pyruvate through two steps catalysis with two enzymes involved, pyruvate decarboxylase (PDC) and alcohol dehydrogenase (ADH, Fig. 1). The product of pyruvate decarboxylase, acetaldehyde is toxic to the cells. Therefore, it is challenging to get engineered strains with strong promoter driving this pathway. However, it is desirable to have high gene expression for higher yield. In this case, an inducible promoter is required. P*nrsB* is induced by Ni^{2+} and Co^{2+} and has been used for e.g. manoyl oxide production in *Synechocystis*[111]. P*nrsB* is part of the *nrsBACD* operon, which encodes Ni^{2+}, Co^{2+} and Zn^{2+} resistant enzymes[112].

To get started, P*nrsB* activity in *Synechocystis* was determined by cloning enhanced yellow fluorescent protein (EYFP) gene[113] after it on the shuttle vector pPMQAK1, resulting in engineered strain PnrsB_EYFP (Table 2, paper III). The *Synechocystis* strain carrying the empty pPMQAK1 vector was the reference strain (empty, control strain in paper I, WT+Km^r-vector in paper II). Chemical $NiCl_2$ was used to induce P*nrsB* when required.

The fluorescence measurements showed that without induction, there was low expression of EYFP in PnrsB_EYFP cells cultivated in BG11 and BG11 without Co^{2+} (Fig.13A). This may due to a leaky promoter (in BG11 without Co^{2+}), trace amount of Co^{2+} in the medium (in BG11) or the combined effects of the two (in BG11). With $NiCl_2$ induction, the effects of different $NiCl_2$ concentrations on the growth and fluorescence were examined. The cells could tolerate 2.5μM Ni^{2+} under the experimental conditions. With higher concentration, the cells stopped growing (Fig. 13B). However, the fluorescence per cell was the highest when 5μM Ni^{2+} was used and was stable when higher concentrations of Ni^{2+} was applied (Fig. 13A). The results imply that P*nrsB* can be used as an inducible promoter for synthetic biology in *Synechocystis* and 2.5 μM Ni^{2+} might be a good concentration.

Furthermore, ethanol was used as another report to test the P*nrsB* in *Synechocystis*. PDC gene (*pdc* from *Zymomonas mobilis*) and ADH gene (*slr1292* from *Synechocystis*) were cloned in one operon driven by P*nrsB* on the shuttle vector pPMQAK1. The resulting *Synechocystis* strain was PnrsB_EtOH (Table 2, paper III). Ethanol production was measured with different concentrations of $NiCl_2$ added. The *Synechocystis* strain carrying the empty pPMQAK1 vector was the reference strain (empty, Table 2, paper III).

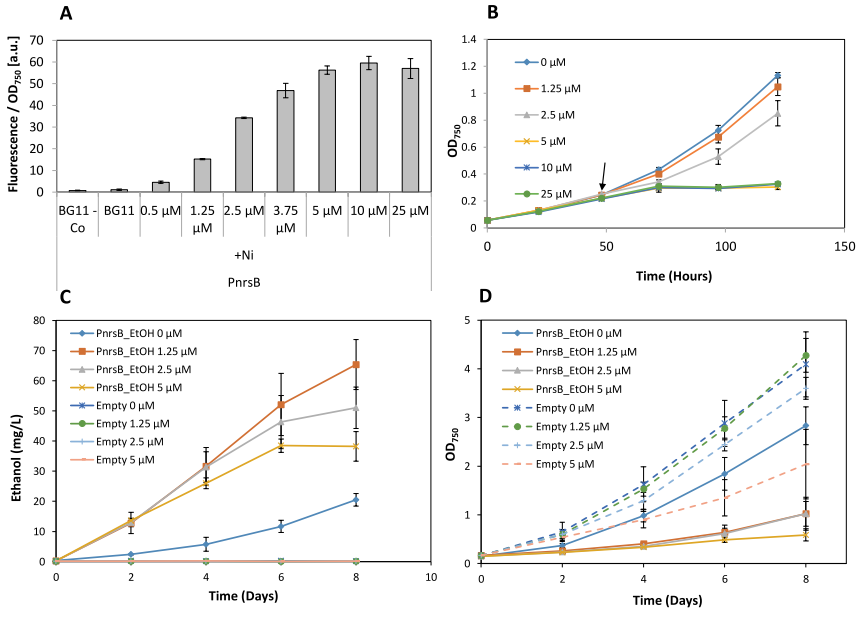

Figure 13. The fluorescence of *Synechocystis* strain PnrsB_EYFP, normalized to OD_{750} after 48 hours of induction (A) and growth of *Synechocystis* strain PnrsB_EYFP, induced by varied concentrations of $NiCl_2$ after 48 hours of inoculation (B). The error bars are the standard deviations from four replicates (A) and triplicates (B). Ethanol production (C) and growth (D) of the empty strain and PnrsB_EtOH strain with P*nrsB* induced by different concentrations of $NiCl_2$. Ni^{2+} was added at the beginning of the cultivation. The error bars are the standard deviations from four replicates. For strain details, see Table 2. The figure is modified from paper III.

In the empty strain, no ethanol was detected no matter how much Ni^{2+} was added (Fig. 13C). The empty strain can tolerate 1.25µM Ni^{2+}. Adding more than 1.25µM Ni^{2+} had negative effects on the growth (Fig. 13D). This effect may be due to the effects of Ni^{2+} on cell metabolism. For strain PnrsB_EtOH, there was low ethanol production when no Ni^{2+} was added (Fig. 13C), which was consistent with the detected low fluorescent signal in strain PnrsB_EYFP when no Ni^{2+} was added (Fig. 13A). Cells produced highest ethanol when 1.25µM Ni^{2+} was added, followed by 2.5µM Ni^{2+} and 5µM Ni^{2+} (Fig. 13C). The ethanol yield was more than 3 times higher in the 1.25µM Ni^{2+} added cultures than that without Ni^{2+} added. Considering growth, negative effects on the PnrsB_EtOH strain were observed when 1.25µM Ni^{2+} was added. When 2.5µM Ni^{2+} was used, similar growth rate was observed as when 1.25µM Ni^{2+} was used, while the growth almost stopped when 5µM Ni^{2+} was used (Fig. 13D). This means the PnrsB_EtOH strain can tolerate lower concentration of Ni^{2+} (1.25µM) compared to the PnrsB_EYFP strain (2.5µM). This may be because the growth of the PnrsB_EtOH strain was affected both by the ethanol and Ni^{2+}. However, the

growth of the PnrsB_EYFP strain is mainly affected by Ni^{2+}, while the EYFP did no have obvious effects on cell growth. These results indicate that P*nrsB* as an inducible promoter can work well to produce ethanol in *Synechocystis* and 2.5μM $NiCl_2$ is one of the good induction concentrations.

This work established an ethanol producing strain PnrsB_EtOH and showed that P*nrsB* can be used as an inducible promoter in *Synechocystis*.

Ethanol production in CBB cycle engineered *Synechocystis* strains (paper IV)

One of the goals of engineering the CBB cycle is to increase the production of carbon compound. As photoautotrophic organisms, cyanobacteria could survive with carbon dioxide, which goes into the cyanobacteria biological cycle through the CBB cycle, as the solo carbon source. Enhancing the efficiency of the CBB cycle would theoretically increase the carbon input, and potentially increase the desired compound yield subsequently. It has been demonstrated that increasing the protein levels of one of the four CBB cycle enzymes, RuBisCO, FBP/SBPase, FBA and TK, led to enhanced growth and/or DCW accumulation under certain experimental conditions (paper I). The production of desired compound (ethanol as an example) was investigated in the CBB cycle engineered strains.

An ethanol producing strain was established (strain PnrsB_EtOH, paper III, EtOH hereafter). Starting from this strain, four more strains were constructed, co-overexpressing one the four CBB cycle enzymes RuBisCO, FBP/SBPase, TK and FBA with the ethanol synthesis cassette on the shuttle vector pPMQAK1. The four strains were named EtOH-rbcSC (with RuBisCO co-overexpressed), EtOH-70glpX (with FBP/SBPase co-overexpressed), EtOH-tktA (with TK co-overexpressed) and EtOH-fbaA (with FBA co-overexpressed, Table 2, paper IV). The expressing genetic constructs in the four strains are illustrated in Figure 14. Again, the strain carrying the empty vector was the reference strain (the control strain).

It was demonstrated that the P*nrsB* had weak expression in BG11, while it had much higher expression when $NiCl_2$ was used for induction (Fig. 13A, paper III). In this study, the condition without Ni^{2+} added was used to test the effects of overexpressing the CBB cycle enzymes on desired compound yield when the desired compound synthesis pathway was not efficiently expressed. The condition with 2.5μM Ni^{2+} added was used to test the effects when the desired compound synthesis pathway was efficiently expressed. To determine the ethanol production, the engineered strains were cultivated in the sealed tissue flasks with 50mM $NaHCO_3$ and 40mM HEPES-NaOH (pH 7.5) under 60μmol photons m^{-2} s^{-1} light intensity.

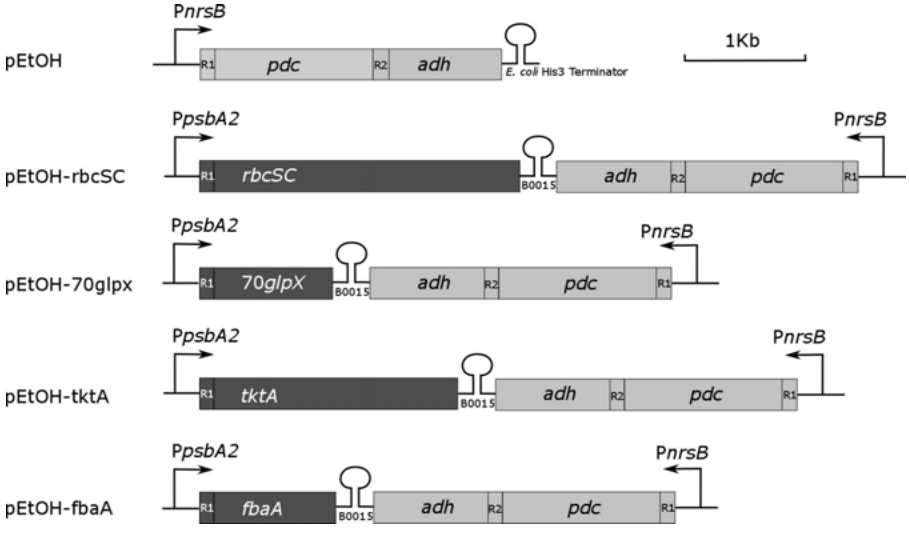

Figure 14. The genetic constructs expressing ethanol synthesis pathway alone (pEtOH) or co-overexpressing one of the four CBB cycle enzymes with the ethanol synthesis pathway (the last four). *pdc*, the pyruvate decarboxylase gene from *Zymomonas mobilis*. *adh*, the alcohol dehydrogenase gene (*slr1192*) from *Synechocystis*. *rbcSC*, the RuBisCO gene from *Synechocystis* with FLAG tag on the C terminus of the small subunit. *70glpX*, the FBP/SBPase gene from *Synechococcos* PCC 7002. *tktA*, the TK gene from *Synechocystis*. *fbaA*, the class II FBA gene from *Synechocystis*. R means ribosome binding site. For strain details, see Table 2. The figure is from paper IV.

When Ni^{2+} was added, the control strain grew faster while the EtOH strain grew the second fast (Fig. 15A). For ethanol production, the control strain barely produced ethanol and the EtOH strain produced less than the EtOH-rbcSC, EtOH-70glpX, EtOH-tktA and EtOH-fbaA strains (Fig. 15C, Table 2, paper IV). This means co-overexpressing the CBB cycle enzymes increases the ethanol production under this condition. On day 7, the EtOH-rbcSC, EtOH-70glpX, EtOH-tktA and EtOH-fbaA strains accumulated 55%, 67%, 37% and 69% more ethanol than the EtOH strain (Fig. 15C).

However, similar results were not observed when no Ni^{2+} was added to the culture. Without Ni^{2+} added, the EtOH strain grew faster than the CBB cycle enzyme co-overexpressed strains at the beginning of the cultivation. However, the EtOH strain stopped growing at early stage, while the other ethanol producing strains kept growing (Fig. 15B). For ethanol production, the EtOH-rbcSC, EtOH-70glpX, EtOH-tktA and EtOH-fbaA strains produced only 2% of the ethanol produced by the EtOH strain (Fig. 15D). This means co-overexpressing the CBB cycle enzymes does not increase the ethanol production under this condition.

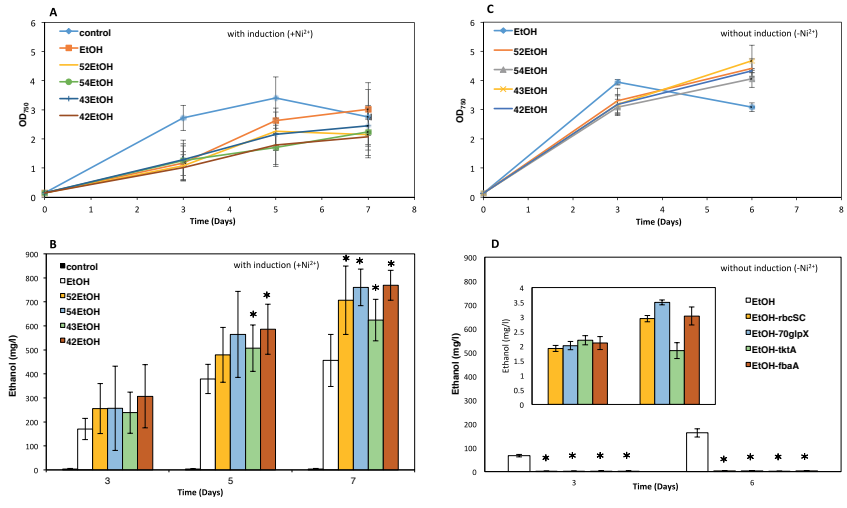

Figure 15. Growth and ethanol production of the engineered *Synechocystis* strains cultivated with and without Ni^{2+} added. The error bars are standard deviations from six biological replicates (A and C) or triplicates (B and D). Asterisks indicate significant difference ($P<0.05$) between the EtOH strain and the other ethanol producing strains according to one-way ANOVA analysis. For strain details, see Table 2. The figure is from paper IV.

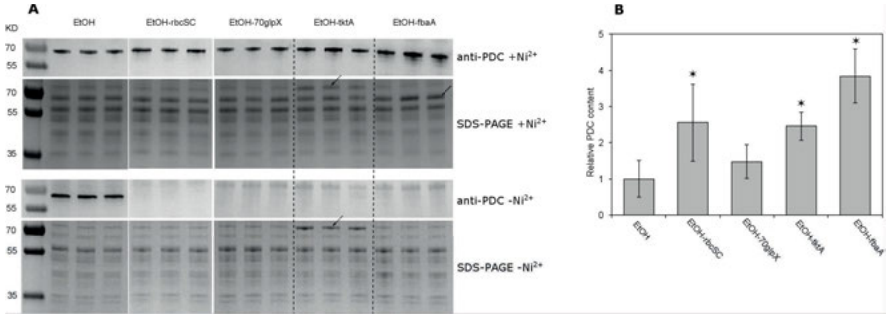

Figure 16. The SDS-PAGE (middle upper and lower panels) and Western immunoblot (upper and middle lower panels) using antibodies against the PDC of cells cultivated with and without Ni^{2+} added (A). The solid arrow indicates the PDC band on the SDS-PAGE. The dotted arrows indicate the TK band on the SDS-PAGE. The upper and middle upper panels are samples with Ni^{2+} added ($+Ni^{2+}$). The lower and middle lower panels are samples without Ni^{2+} added ($-Ni^{2+}$). The relative PDC amount in the engineered strains standardized to the reference strain calculated with the Quantity-One (B). The error bars are standard deviations from biological triplicates and technical replicates. Asterisks indicate significant difference ($P<0.05$) between the EtOH strain and the other ethanol producing strains according to one-way ANOVA analysis. For strain details, see Table 2. The figure is modified from paper IV.

To understand the relationships between the PDC level and the ethanol formation, the PDC level was detected in the cells. The results showed that

the PDC level was consistent with the ethanol yield under conditions with and without Ni^{2+} added (Fig. 16). With Ni^{2+} added, the EtOH-rbcSC, EtOH-70glpX, EtOH-tktA and EtOH-fbaA strains produced more ethanol (Fig. 15B) and had more PDC compared to the EtOH strain (Figs. 16A and 16B). Without Ni^{2+} added, it was opposite, meaning the EtOH strain produced more ethanol (Fig. 15D) and had more PDC (Fig. 16A).

Under the condition with Ni^{2+} added, the results of the dry cell weight (DCW) and growth were consistent (Figs. 15A and 17A). The control strain accumulated the highest DCW, while the EtOH strain was the second high (Fig. 17A). But none of these differences are statistically significant. In contrast, the total biomass (ethanol plus DCW) accumulation was higher in the CBB cycle enzyme co-overexpressed strains than in the EtOH strain, while the EtOH strain was higher than the control strain (Fig. 17B). At the end of the cultivation, the total biomass of the EtOH strain was 38.8% higher than the control strain. This was consistent with the report in *Synechococcus elongatus* PCC 7942, where putting an efficient carbon sink (sucrose) increased the biomass accumulation[114]. The total biomass in EtOH-rbcSC, EtOH-70glpX, EtOH-tktA and EtOH-fbaA strains was further increased, 7.7%, 15.1%, 8.8% and 10.1% higher compared to that in the EtOH strain, respectively (Fig. 17B). The ethanol producing strains formed more ethanol (Fig. 15C), accumulated more total biomass (Fig. 17B) but less DCW (Fig. 17A). Thus it was clear that the ethanol producing strains accumulated more total biomass than the control strain in the form of ethanol. In the EtOH strain, the ethanol to total biomass ratio was 30.2% at the end of the cultivation, while in EtOH-rbcSC, EtOH-70glpX, EtOH-tktA and EtOH-fbaA strains, it increased to 43.6%, 45.2%, 38.4% and 47.4%, respectively (Fig. 17C).

Different results were obtained when no Ni^{2+} was added. The EtOH-rbcSC, EtOH-70glpX, EtOH-tktA and EtOH-fbaA strains had higher DCW but slightly lower total biomass compared to the EtOH strain (Figs. 17D and 17E). Taking the ethanol production into consideration (Fig. 15D), it implies that the EtOH strain directed some carbons to ethanol production, but the CBB cycle enzyme co-overexpressed strains directed almost all the carbons to the DCW accumulation since there was barely ethanol production. This led to the results that the ethanol to the total biomass ratio was much lower in the CBB cycle enzyme co-overexpressed strains compared to that in the EtOH strain (Fig. 17F).

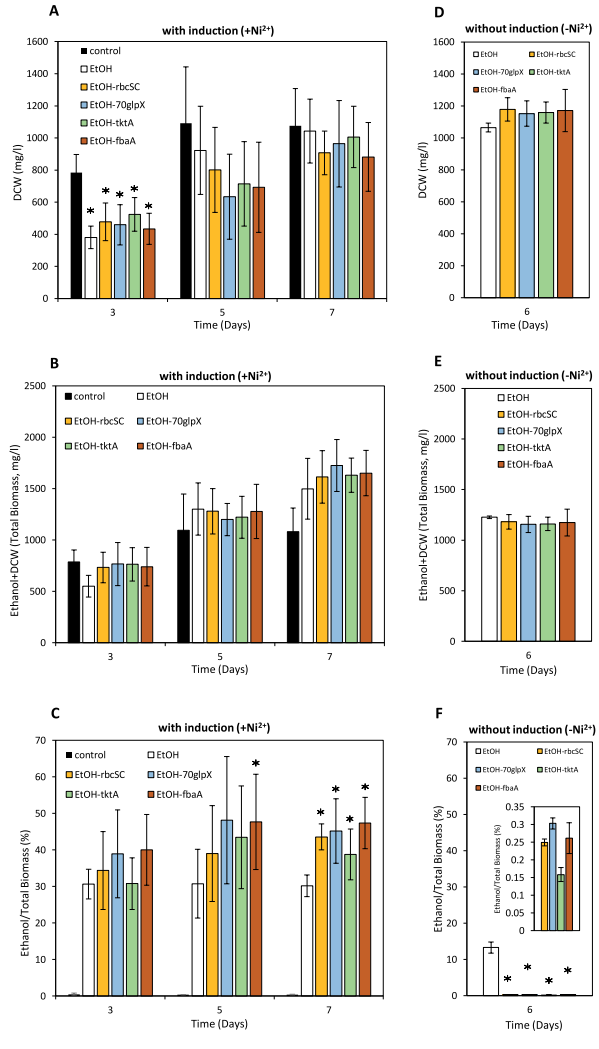

Figure 17. The DCW, total biomass (DCW and ethanol) and ethanol to total biomass ratio of engineered *Synechocystis* strains with (A, B and C) and without (D, E and F) 2.5μM Ni^{2+} added. Error bars are standard deviations from six (A, B and C) and three (D, E and F) biological replicates. Asterisks indicate significant difference ($P<0.05$) between the EtOH strain and the CBB cycle enzyme co-overexpressed strains according to one-way ANOVA analysis. For strain details, see Table 2. The figure is from paper IV.

Co-overexpressing the CBB cycle enzymes with the ethanol synthesis cassette increased the ethanol production only when the ethanol synthesis cassette promoter P*nrsB* was induced, meaning that the ethanol synthesis pathway was effectively expressed. Besides, introducing an efficient sink into cells has positive effects on biomass (or total biomass) accumulation.

Conclusion and Outlook

As the main carbon fixation cycle in nature, the CBB cycle attracts intensive attentions to mitigate the climate change and to produce sustainable resources for variable usages. The CBB cycle uses RuBisCO, one of the most inefficient enzymes in nature, as the carboxylase. Because of the slow turnover rate and the competitive oxygenase activity, RuBisCO was regarded as the main rate-limit step in the CBB cycle for a long time. However, combining the biochemical analysis on the enzyme kinetics and analysis of the metabolic flux in antisense transgenic plants, SBPase, FBA and TK, together with RuBisCO, are potential carbon flux control enzymes in the CBB cycle in plants[8,9].

In this thesis, effects of the CBB cycle engineering on the growth and desired compound forming in the model cyanobacterium *Synechocystis* PCC 6803 was studied. Four of the CBB cycle enzymes, RuBisCO, FBP/SBPase, FBA or TK were overexpressed in the wild type cells individually. Targeting on RuBisCO overexpression, two methods showed positive effects on the detected RuBisCO level. One method was to introduce a second copy of the carboxysome protein CcmM gene into the cells. The results imply that the carboxysome protein CcmM may help to stabilize RuBisCO by localizing it into the carboxysome. The other method was to tag the RuBisCO protein with FLAG either on the N terminus of the large subunit or on the C terminus of the small subunit on shuttle vector. The FLAG tag has positive effects on the detected RuBisCO level, but not the specific RuBisCO activity. For FBP/SBPase, it was easy to see the overexpression on the SDS-PAGE gels when a second copy of gene, native from *Synechocystis* PCC 6803 or heterologous from *Synechococcus elongatus* PCC 7942 and *Synechococcus* PCC 7002, was introduced into the wild type cells. A second copy of the class I FBA and class II FBA genes from *Synechocystis* PCC 6803 were introduced into the wild type cells on the shuttle vector separately. The class II FBA was overexpressed based on the SDS-PAGE results, while it was difficult to see the overexpression of class I FBA. Like FBP/SBPase, the overexpression of TK was clear on the SDS-PAGE gels when a second copy of gene was introduced into the wild type cells.

As the results of the CBB cycle engineering, enhanced growth, biomass accumulation and net oxygen evolution rate measured under saturated light condition were observed in the strains with RuBisCO, FBP/SBPase or FBA overexpressed when cultivated under 100μmol photons m^{-2} s^{-1}. The strain

with TK overexpressed accumulated more biomass under the same experimental conditions, but grew slower and had decreased oxygen evolution rate. The inconsistency between the biomass and growth may have something to do with the cell volume. More data are required to elucidate the reasons. On the base of positive effects of the CBB cycle enzymes overexpressed, the effects on a desired compound (ethanol as an example in this thesis) yield were investigated in these strains. When the ethanol synthesis pathway was efficiently expressed in the CBB cycle engineered strains, the ethanol yield increased compared to the strain with non-engineered CBB cycle. Besides, in the CBB cycle engineered strains, almost 50% of the fixed carbon directed to the desired compound, ethanol formation. Conclusively, the four enzymes studied in this thesis have controls over the CBB cycle carbon flux in *Synechocystis* PCC 6803 and overexpressing them individually has positive effects on compound production.

To understand the reasons to the phenomenon after the protein overexpressed, a lot more experiments are required. For example, the increase of net oxygen evolution measured under saturated light condition implies changes in water splitting efficiency of PSII. Consequently, this might have effects on the entire photosystem, and the ATP & NADPH content in cells. These two components play important roles in the whole metabolism. Therefore, getting the carbon flux maps of the engineered strains will be useful to understand the reasons to the effects and valuable for more complete cyanobacterial models to guide the engineering strategies. Besides, the different engineered strains showed similar phenotypes even though the overexpression levels varied. In this case, it is possible that the restrictions shift to other reaction(s). It is also possible that the cells regulate and balance protein activities in certain way(s). The highly overexpressed proteins, like the FBP/SBPase in fbpI strain (Figs. 3B and 3D), may not be fully activated. Therefore, delicate gene expression systems in cyanobacteria are highly required to investigate the balance points.

Fixing carbon into desired compounds by biological methods, like presented in this thesis, chemical methods[115] and through electrosynthesis[116–118] are all rapidly developing. For biological carbon fixation, both native fixing pathways *in vivo* and artificial pathways *in vitro* are being investigated[79,81]. Besides, introducing CO_2 utilization pathways into heterotrophic cells could also increase the yield of desired compounds[119]. All these strategies are promising to get valuable compounds effectively from atmospheric CO_2.

Except for carbon fixation efficiency, the overall solar energy conversion efficiency is another important factor affecting the production in photosynthetic organisms. These organisms use antenna to absorb and transfer solar energy to the photochemical reaction center. During this process, the excess solar energy is dissipated as heat. This often happens in the leaves on the top of the canopies and cells in the surface facing the light source of the algae and cyanobacteria dense cultures. However, the leaves on the bottom of the

canopies and the cells not on the surface facing the light source of the algae and cyanobacteria cultures will not get enough solar source. As a result, the energy conversion efficiency of the population is reduced. Therefore, a strategy, using "truncated light-harvesting antenna (TLA)", was developed and used in plants, algae and cyanobacteria to increase the total solar energy conversion efficiency[120,121]. This strategy is to decrease the antenna size to prevent the top leaves and cells to absorb excess solar energy and allow the lower leaves and cells to receive more solar energy. In this way, the light inhibition of the top leaves and cells is mitigated, while the lower leaves and cells accept more solar energy. As a result, the overall solar energy conversion efficiency and production will be enhanced.

The carbon fixation and light harvesting engineering can be combined with the engineering of the specific synthetic pathway of a certain compound to achiever a higher yield. The engineering can use natural existing pathways in native or heterologous host or artificial pathways with new reactions or/and new enzymes[122]. Besides, extracting the compound out of the cells during the cultivation may also have positive effects on the photosynthesis or/and carbon fixation[95,96]. Since the organisms usually evolve in a way to achieve maximum growth instead of benefiting compound formation, the combined engineering on photosynthesis, carbon fixation and specific compound synthetic pathway may direct more energy and carbon source to the compound formation instead of growth.

Sammanfattning på Svenska

Jämfört med medeltemperaturen på jorden mellan 1951 och 1980 har temperaturen idag ökat med nästan 1 °C. Den atmosfäriska koldioxidnivån har precis passerat 400 ppm, cirka 30 procent högre än den var under industriella revolutionen. Koldioxid är en av växthusgaserna som fångar solvärme på jorden och bidrar till den globala uppvärmningen. Förbränningen av fossila bränslen är den huvudsakliga orsaken till ökningen av koldioxidnivåerna i atmosfären. Vi behöver minska användningen av fossila tillgångar och samtidigt utveckla förnybara bränslen som skapas från den koldioxid som redan är en del av kolets kretslopp. Ett av de främsta sätten att minska mängden koldioxid i atmosfären är genom biologisk kolfixering genom en process vi kallar fotosyntes. Man har uppskattat att enzymet ribulos-1,5-bisfosfatkarboxylas/oxygenas (RuBisCO), som är det primära enzymet kolfixerande enzymet i fotosyntesen, fixerar flera miljarder ton koldioxid per år, vilket motsvarar ungefär 90% av all fixerat kol. RuBisCO är ett av nyckel enzymerna i Calvin-Benson-Bassham (CBB) cykeln, den huvudsakliga kolfixerande cykeln i naturen och därmed också med en viktig roll i jordens kolkretslopp. CBB cykeln, också kallad mörkerreaktionen, bildar tillsammans med ljusreaktion fotosyntesen, vilken därmed är den avgörande processen för att fixera koldioxid i atmosfären och lagra solenergi i kemisk form. Organiskt material kan efter långvarig förvaring i marken omvandlas till fossila bränslen, vilka är de främsta energikällorna vi använder idag. Men användningen av kol och olja släpper ut stora mängder koldioxid och andra gaser och orsaka därmed miljöförstöringar. Dessutom så tar den naturliga framställningen av fossila resurser många miljoner år, vilket gör det omöjligt att tillgodose det snabbt växande globala energibehovet. Utöver det ökande behovet av bränsle så är det framtida behovet av mat en annan utmaning. År 2050 kommer den globala matkonsumtionen ha ökat med mer än 50%. För att minska användandet av fossila bränslen och öka matproduktionen forskas det på att skapa förnybara bränslen direkt från solens energi genom olika organismer. Från den forskningen har produktion av värdefulla ämnen direkt från fotosyntetiska cyanobakterier visat sig vara en lovande framtidsteknologi.

Cyanobakterier är gröna bakterier med fotosyntes som uppkom för flera miljarder år sedan. De är de mikroorganismer som bidrog till att ändra atmosfären från att vara helt syrefri till att innehålla syre, bildat i ljusreaktionen av den fotosyntetiska processen. Precis som växter kan cyanobakterier om-

vandla koldioxid från luften till organiska föreningar genom att förbruka vatten och solenergi. Dessutom har cyanobakterier fördelarna gentemot växter att det är relativt lätt att ändra deras arvsmassa samt att de har en kort livscykel. Därför kan cyanobakterier med modern genteknik omvandlas till ”cellfabriker” som använder solenergi för att producera specifika kemikalier och ämnen användbara för samhället. I naturen använder cyanobakterier enzymet RuBisCO för att fixera koldioxid, ett ensym som är förvånansvärt ineffektivt. Forskare har försökt modifiera RuBisCO för att förbättra dess egenskaper men till exempel varje modifikation som ökar hastigheten på enzymet minskar dess affinitet till koldioxid, det vill säga enzymet arbetar snabbare men attraktionskraften att binda koldioxid minskar. Istället kan attraktionskraften att binda syrgas, den negativa oxygenasreaktionen av enzymet, öka. Den låga effektiviteten hos RuBisCO och CBB cykeln är ett hinder för en effektiv fotosyntes, inklusive en framtida produktion av värdefulla ämnen och molekyler från cyanobakterier. Därför är det viktigt att försöka förbättra dessa organismers kolfixering så de blir mer produktiva. Av de elva enzymerna i CBB cykeln så har fyra av dem, RuBisCO, SBPase, FBA och TK, i växterstudier visat sig speciellt viktiga för att kontrollera och reglera den kolfixerande processen.

I den här avhandlingen har de fyra tidigare identifierade, speciellt viktiga nyckelenzymerna i CBB cykeln, RuBisCO, SBPase, FBA och TK, studerats i den encelliga cyanobakterien *Synechocystis* PCC 6803. Genom att använda genteknik, delvis också utvecklad inom avhandlingsarbetet, så skapades genmodifierade stammar som har en ökad mängd av respektive enzym. Vid lågt ljus utvecklade de stammarna mer syre från fotosyntesen och vid högre ljus växte de dessutom fortare. Högre tillväxt betyder bland annat att de fixerar mer koldioxid. För att se om de här genmodifieringarna kan användas för att fixera mer koldioxid till en specifik produkt modifierades några nya stammar till att förutom att ha en ökad mängd CBB enzymer, och därmed också en ökad tillväxt, också producera etanol. Etanol är ett exempel på ett ämne, en kemikalie eller ett bränsle, som man med modern genteknik kan få cyanobakterier att producera i direkta processer. Resultaten från studien visade att de modifierade stammarna kan tillverka upp till 70% mer etanol än en kontrollstam som har mer normala mängder CBB enzymer. Dessutom bildade de upp till 15% mer biomassa vilket indikerar att de fixerar betydligt mer koldioxid. Studien visar att det är möjligt att optimera CBB cykeln för ökad tillväxt och produktionen av specifika produkter. Fler experiment behövs för att bättre förstå vad som verkligen händer i cellerna när de fixerar med koldioxid, t.ex. om en ökad mängd av ett specifikt CBB nyckelenzym påverkar mängden av de andra enzymerna i cykeln, hur det påverkar förekomsten av andra ämnen i cellen samt var flaskhalsen för maximal produktion är.

I naturen är CBB cykeln inte den enda kolfixerande processen och inte heller den mest effektiva. Det finns fem andra identifierade naturliga kolfixe-

rande reaktionsvägar och några av dem är mer effektiva än CBB cykeln. Trots det har naturen valt den mindre effektiva CBB cykeln som den huvudsakliga kolfixerande processen. Genom att använda datamodeller har artificiella kolfixerande reaktionsvägar identifierats som potentiellt ska ha ännu fördelaktigare egenskaper. Det finns inga organismer som innehåller dessa helt syntetiska metaboliska flöden, det vill säga evolutionen har inte utvecklat dem. Däremot finns de enskilda stegen i de olika metaboliska flödena i någon organism. Att sätta samman de olika reaktionerna till ett helt metaboliskt flöde, en ny metabolism, i en levande cell är nästa stora utmaning. En djupare förståelse för CBB cykeln kan bidraga till att lösa den utmaningen. Det finns fortfarande många aspekter av CBB cykeln där kunskapen inte är tillräckligt stor, som dynamik och kinetik av de olika ingående enzymerna, de biologiska funktionerna av intermediära metaboliterna, regleringen av cykeln under olika yttre förhållanden samt effekten av att ändra mängderna av enzymer i cykeln. Resultaten från den här avhandlingen ger oss en bättre förståelse för CBB cykeln, identifierar några sätt att öka kolfixeringen, och därmed tillväxten, och kan på så sätt stimulera till en fortsatt utveckling av cyanobakterier som ”framtidens gröna cellfabriker”.

Acknowledgement

Time flies. I had good time in Uppsala and it was exciting to experience different cultures. After more than four years, this moment comes. To set this milestone of my life, both an end and a beginning, I would like to give the credits to many people.

So many thanks go to my main supervisor **Peter Lindblad**. You offered me this precious opportunity to do my PhD in Uppsala University. You were so supportive and gave me absolute freedom doing research. It is not only the knowledge that you delivered is treasure to me, but also your positive attitudes toward life, which helps me to conquer many research difficulties.

Thanks to my co-supervisor **Pia Lindberg**. It is surprisingly enjoyable to talk to you because of your patience and humor. It is lucky for me to have you as my supervisor. You are knowledgeable and always give straightforward and logical solutions to research problems, which make my PhD study much easier and more promising.

Thank you, **Karin Stensjö**. You are energetic and encouraging so it is always nice to talk to you to cheer us up. You have the magic to let us believe that everything is going to be fine and calm us down to focus on whatever we need to do to achieve this.

I would like to thank all the other lovely colleagues of the cyano group also. **Rui Miao**, the second person I know from the cyano group except my main supervisor. You are the "catalyst" for me to decide to come to Uppsala and it turned out that I made the right decision. You helped me to start the life in Uppsala and kept helping me to solve any problems afterwards. I am really grateful.

Claudia Durall, the person who helped me to start the lab works. I appreciate all the helps from you on my private life and all the jokes and good times (e.g. hiking in Golden) spending together. You look "gorgeous" when you were dancing on the table.

Elias Englund, for the excellent organizations of group salary lunches/dinners and Christmas parties, and the excellent advices on lab works. Besides, thank you so much for translating the thesis summary into Swedish.

Adam Wegelius, for the good suggestions of outdoor activities, the excellent "shows" after you were drunk and all the "annoying" talks.

Xin Li, for the suggestions of good chicken wings in Uppsala.

Xufeng Liu, for the good times and memories. It has been years.

Christoph Howe, for all the knowledgeable talks.

Dennis Dienst, Kateryna Kukil, and João Rodrigues, for giving me the chance to know three amazing scientists short before my graduation.

Thanks to the people who ever worked in the cyano group. **Namita Khanna**, you are one of the kindest people I know in my life. I hope we will have another chance to have "Friday dinner" together somewhere in the world.

Bagmi Pattanaik, you are amazing at taking care of the lab affairs and after party messes. I am still wondering how can you be satisfied with such small amount of lunch.

Daniel Camsund, for all the inspiring ideas. You are a good scientist and I believe that you will make it better.

Many thanks to other colleagues working and worked in the cyano group. **Hao Xie, Inés Varela, Katja Annala, Giovanni Barone, Isabel Moreno de Palma, Simon Eklöv, Robin Hoheneder, Federico Turco, Ingrid Lekberg Osterman**, thanks for making such a nice working environment and all the best for your futures.

I am grateful for the companies of people in the neighbor group, still here or left for a new life journey, **Felix Ho**, **Ann Magnuson**, **Ping Huang**, **Fikret Mamedov**, **Gustav Berggren**, **Nigar Ahmadova**, **Livia Meszaros**, **Brigitta Németh**, and **Patrícia Raleiras**. Thanks you all and I will remember all the good times.

Thank the professors **Jan**, **Johannas**, **Stenbjö**, and **Leif** to make the department of chemistry-Ångström an excellent place to do science.

Thank you, **Jessica Stålberg**, for taking care of the receipts, shocking us with all the amazing decoration ideas, and giving me the great chance to know your lovely boys. **Susanne Söderberg**, for the helps with study proof and so many other proofs. I am going to miss the good morning wish forever. **Sven Johansson**, for taking care of our lab equipment, consumable lab materials, and the amazing introductions on the old cars.

I also thank the companies of other colleagues from the department of chemistry-Ångström, **Shihuai Wang, Tianfei Liu, Ruisheng Xiong, Jing Huang** (a good company to go to swimming pool)**, Rabia Ayub, Huimin Zhu** (a good company to swim and play ping pang even though we are not going very often recently)**, Liyang Shi** and **Lei Tian**.

Great thanks go to all the other friends in Uppsala. **Lichuan Wu, Shunguo Wang, Changqing Ruan** (a great chef and a good ping pang partner), **Meiyuan Guo, Yuhan Ma** (I never knew that a person can be so happy after buying new lip sticks)**, Fengzhen Sun, Jiajie Yan, Liguo Wang, Weijia Yang, Michelle Edel Nordkvist** (an outdoor expert. It is always relax to talk to you)**, Lingyan Zhang** (my lovely flat mate), **Kai Song** (another chef I met in Uppsala), **Shiyu Li** (I have to say the French movies were so boring), **Xingxing Xu**, **Shuangshuang Zeng** (Next time, say something nice please) and **Chenyu Wen**. Thanks for being here to make my Uppsala life great. I wish you guys all the best.

Thank the Chinese scholarship (CSC) to support my study in Uppsala University and the Liljewalchs, Åforsk, and Anna Maria Lundins travel scholarships to finance me to attend international conferences and visit collaboration labs.

Thanks to my master supervisor, **Xuefeng Lv**, mentor **Xiaoming Tan**, and my previous senior colleagues **Lun Yao** and **Xuenian Huang**. Thanks for helping me to get started with the scientific research life and keeping supporting me all the way till now. I wish good lucks to your careers and lives. Great thanks also go to my beloved friends since university, **Jiayi Qin**. You said after more than 10 years of being friends, we are already family and I truly think so.

At last, I appreciate the loves and supports from my parents, my sister, my aunt and my uncle. Your loves make every step for me easier and motivate me to keep moving forward. I wish you all a happy and healthy life and I will do whatever it takes to make this come true.

References

1. Melorose, J., Perroy, R. & Careas, S. World population prospects. *United Nations* **1,** 587–92 (2015).
2. Ray, D. K., Mueller, N. D., West, P. C. & Foley, J. A. Yield Trends Are Insufficient to Double Global Crop Production by 2050. *PLoS One* **8,** (2013).
3. Soo, R. M., Hemp, J., Parks, D. H., Fischer, W. W. & Hugenholtz, P. On the origins of oxygenic photosynthesis and aerobic respiration in Cyanobacteria. *Science.* **355,** 1436–1440 (2017).
4. Planavsky, N. J. *et al.* Evidence for oxygenic photosynthesis half a billion years before the Great Oxidation Event. *Nat. Geosci.* **7,** 283–286 (2014).
5. Schirrmeister, B. E., Gugger, M. & Donoghue, P. C. J. Cyanobacteria and the Great Oxidation Event: evidence from genes and fossils. *Palaeontology.* **58,** 769–785 (2015).
6. Martin, W. *et al.* Evolutionary analysis of Arabidopsis, cyanobacterial, and chloroplast genomes reveals plastid phylogeny and thousands of cyanobacterial genes in the nucleus. *Proc. Natl. Acad. Sci. USA.* **99,** 12246–12251 (2002).
7. Raven, J. A., Beardall, J. & Sánchez-Baracaldo, P. The possible evolution, and future, of CO_2-concentrating mechanisms. *J. Exp. Bot.* **68,** 3701–3716 (2017).
8. Raines, C. A. The Calvin cycle revisited. *Photosynth. Res.* **75,** 1–10 (2003).
9. Zhu, X.-G., de Sturler, E. & Long, S. P. Optimizing the distribution of resources between enzymes of carbon metabolism can dramatically increase photosynthetic rate: A numerical simulation using an evolutionary algorithm. *Plant Physiol.* **145,** 513–526 (2007).
10. Kaneko, T. *et al.* Sequence analysis of the genome of the unicellular cyanobacterium *Synechocystis* sp. strain PCC 6803. II. Sequence determination of the entire genome and assignment of potential protein-coding regions. *DNA Res.* **3,** 109–136 (1996).
11. Kerfeld, C. A. & Melnicki, M. R. Assembly, function and evolution of cyanobacterial carboxysomes. *Curr. Opin. Plant Biol.* **31,** 66–75 (2016).
12. Cameron, J. C., Wilson, S. C., Bernstein, S. L. & Kerfeld, C. A. XBiogenesis of a bacterial organelle: The carboxysome assembly pathway. *Cell.* **155,** 1131–1140 (2013).
13. Long, B. M., Tucker, L., Badger, M. R. & Price, G. D. Functional cyanobacterial carboxysomes have an absolute requirement for both long and short forms of the CcmM protein. *Plant Physiol.* **153,** 285–293 (2010).
14. Balsera, M. *et al.* Ferredoxin: Thioredoxin reductase (FTR) links the regulation of oxygenic photosynthesis to deeply rooted bacteria. *Planta.* **237,** 619–635 (2013).
15. Schürmann, P. & Buchanan, B. B. The Ferredoxin/Thioredoxin system of oxygenic photosynthesis. *Antioxid. Redox Signal.* **10,** 1235–1274 (2008).

16. Lindahl, M., Mata-Cabana, A. & Kieselbach, T. The disulfide proteome and other reactive cysteine proteomes: analysis and functional significance. *Antioxid. Redox Signal.* **14,** 2581–2642 (2011).
17. Trost, P. *et al.* Thioredoxin-dependent regulation of photosynthetic glyceraldehyde-3-phosphate dehydrogenase: Autonomous vs. CP12-dependent mechanisms. *Photosynth. Res.* **89,** 263–275 (2006).
18. Tamoi, M., Miyazaki, T., Fukamizo, T. & Shigeoka, S. The Calvin cycle in cyanobacteria is regulated by CP12 via the NAD(H)/NADP(H) ratio under light/dark conditions. *Plant J.* **42,** 504–513 (2005).
19. Michelet, L. *et al.* Redox regulation of the Calvin–Benson cycle: something old, something new. *Front. Plant Sci.* **4,** 1–21 (2013).
20. Fell, D. Understanding the control of metabolism. *Front. Metab.* **2,** 300 (1997).
21. Savir, Y., Noor, E., Milo, R. & Tlusty, T. Cross-species analysis traces adaptation of Rubisco toward optimality in a low-dimensional landscape. *Proc. Natl. Acad. Sci. USA.* **107,** 3475–3480 (2010).
22. Tcherkez, G. G. B., Farquhar, G. D. & Andrews, T. J. Despite slow catalysis and confused substrate specificity, all ribulose bisphosphate carboxylases may be nearly perfectly optimized. *Proc. Natl. Acad. Sci. USA.* **103,** 7246–7251 (2006).
23. Studer, R. A., Christin, P.-A., Williams, M. A. & Orengo, C. A. Stability-activity tradeoffs constrain the adaptive evolution of RubisCO. *Proc. Natl. Acad. Sci. USA.* **111,** 2223–2228 (2014).
24. Sage, R. F. Photosynthetic efficiency and carbon concentration in terrestrial plants: the C4 and CAM solutions. *J. Exp. Bot.* **65,** 3323–3325 (2014).
25. Li, F. W., Villarreal, J. C. & Szövényi, P. Hornworts: an overlooked window into carbon-concentrating mechanisms. *Trends Plant Sci.* **22,** 275–277 (2017).
26. Faulkner, M. *et al.* Direct characterization of the native structure and mechanics of cyanobacterial carboxysomes. *Nanoscale.* **9,** 10662–10673 (2017).
27. Whitney, S. M., Houtz, R. L. & Alonso, H. Advancing our understanding and capacity to engineer nature's CO_2-sequestering enzyme, Rubisco. *Plant Physiol.* **155,** 27–35 (2011).
28. Iwaki, T. *et al.* Expression of foreign type I ribulose-1,5-bisphosphate carboxylase/ oxygenase (EC 4.1.1.39) stimulates photosynthesis in cyanobacterium *Synechococcus* PCC7942 cells. *Photosynth. Res.* **88,** 287–297 (2006).
29. Whitney, S. M., Baldet, P., Hudson, G. S. & John Andrews, T. Form I Rubiscos from non-green algae are expressed abundantly but not assembled in tobacco chloroplasts. *Plant J.* **26,** 535–547 (2001).
30. Hauser, T., Popilka, L., Hartl, F. U. & Hayer-Hartl, M. Role of auxiliary proteins in Rubisco biogenesis and function. *Nat. Plants.* **1,** 15065 (2015).
31. Tabita, F. R., Satagopan, S., Hanson, T. E., Kreel, N. E. & Scott, S. S. Distinct form I, II, III, and IV Rubisco proteins from the three kingdoms of life provide clues about Rubisco evolution and structure/function relationships. *J. Exp. Bot.* **59,** 1515–1524 (2008).
32. Spreitzer, R. J. Role of the small subunit in ribulose-1,5-bisphosphate carboxylase/oxygenase. *Arch. Biochem. Biophys.* **414,** 141–149 (2003).
33. Tabita, F. R. *et al.* Function, structure, and evolution of the RubisCO-like proteins and their RubisCO homologs. *Microbiol. Mol. Biol. Rev.* **71,** 576–599 (2007).

34. Hanson, T. E. & Tabita, F. R. A ribulose-1,5-bisphosphate carboxylase/oxygenase (RubisCO)-like protein from *Chlorobium tepidum* that is involved with sulfur metabolism and the response to oxidative stress. *Proc. Natl. Acad. Sci. USA.* **98,** 4397–4402 (2001).
35. Ashida, H. A functional link between RuBisCO-like protein of bacillus and photosynthetic RuBisCO. *Science.* **302,** 286–290 (2003).
36. Erb, T. J. *et al.* A RubisCO-like protein links SAM metabolism with isoprenoid biosynthesis. *Nat. Chem. Biol.* **8,** 926–932 (2012).
37. Cleland, W. W., Andrews, T. J., Gutteridge, S., Hartman, F. C. & Lorimer, G. H. Mechanism of Rubisco: The carbamate as general base. *Chem. Rev.* **98,** 549–562 (1998).
38. Pearce, F. G. Catalytic by-product formation and ligand binding by ribulose bisphosphate carboxylases from different phylogenies. *Biochem. J.* **399,** 525–534 (2006).
39. Zhang, N. & Portis, a R. Mechanism of light regulation of Rubisco: a specific role for the larger Rubisco activase isoform involving reductive activation by thioredoxin-f. *Proc. Natl. Acad. Sci. USA.* **96,** 9438–43 (1999).
40. Mueller-Cajar, O. *et al.* Structure and function of the AAA + protein CbbX, a red-type Rubisco activase. *Nature.* **479,** 194–199 (2011).
41. Sutter, M. *et al.* Structural characterization of a newly identified component of α-carboxysomes: The AAA+ domain protein CsoCbbQ. *Sci. Rep.* **5,** 1–14 (2015).
42. Tsai, Y. C. C., Lapina, M. C., Bhushan, S. & Mueller-Cajar, O. Identification and characterization of multiple rubisco activases in chemoautotrophic bacteria. *Nat. Commun.* **6,** 1–10 (2015).
43. Lorentzen, E., Siebers, B., Hensel, R. & Pohl, E. Mechanism of the Schiff base forming fructose-1,6-bisphosphate aldolase: Structural analysis of reaction intermediates. *Biochemistry.* **44,** 4222–4229 (2005).
44. Flechner, A., Gross, W., Martin, W. & Schnarrenberger, C. Chloroplast class I and class II aldolases are bifunctional for fructose-1, 6-biphosphate and sedoheptulose-1, 7-biphosphate cleavage in the Calvin cycle. *FEBS Lett.* **447,** 200–202 (1999).
45. Chiadmi, M., Navaza, A., Miginiac-Maslow, M., Jacquot, J. P. & Cherfils, J. Redox signalling in the chloroplast: structure of oxidized pea fructose-1,6-bisphosphate phosphatase. *EMBO J.* **18,** 6809–15 (1999).
46. Serrato, A. J. *et al.* CpFBPaseII, a novel redox-independent chloroplastic isoform of fructose-1,6-bisphosphatase. *Plant, Cell Environ.* **32,** 811–827 (2009).
47. Gütle, D. D. *et al.* Chloroplast FBPase and SBPase are thioredoxin-linked enzymes with similar architecture but different evolutionary histories. *Proc. Natl. Acad. Sci. USA.* **113,** 6779–6784 (2016).
48. Masahiro Tamoi, Toru Takeda, and S. S., Masahiro, T., Takeda, T. & Shigeoka, S. Functional Analysis of Fructose-1,6-Bisphosphatase Isozymes (fbp-I and fbp-II Gene Products) in Cyanobacteria. *Plant Cell Physiol.* **40,** 257–261 (1999).
49. Henkes, S., Sonnewald, U., Badur, R., Flachmann, R. & Stitt, M. A Small Decrease of Plastid Transketolase Activity in Antisense Tobacco Transformants Has Dramatic Effects on Photosynthesis and Phenylpropanoid Metabolism. *Plant Cell.* **13,** 535–551 (2001).
50. Atsumi, S., Higashide, W. & Liao, J. C. Direct photosynthetic recycling of carbon dioxide to isobutyraldehyde. *Nat. Biotechnol.* **27,** 1177–80 (2009).

51. Ruffing, A. M. Borrowing genes from *Chlamydomonas reinhardtii* for free fatty acid production in engineered cyanobacteria. *J. Appl. Phycol.* **25,** 1495–1507 (2013).
52. Ruffing, A. M. Improved free fatty acid production in cyanobacteria with *Synechococcus* sp. PCC 7002 as host. *Front. Bioeng. Biotechnol.* **2,** 1–10 (2014).
53. Lin, M. T., Occhialini, A., Andralojc, P. J., Parry, M. A. J. & Hanson, M. R. A faster Rubisco with potential to increase photosynthesis in crops. *Nature.* **513,** 547–550 (2014).
54. Kanno, M., Carroll, A. L. & Atsumi, S. Global metabolic rewiring for improved CO_2 fixation and chemical production in cyanobacteria. *Nat. Commun.* **8,** 14724 (2017).
55. Ma, W., Shi, D., Wang, Q., Wei, L. & Chen, H. Exogenous expression of the wheat chloroplastic fructose-1,6-bisphosphatase gene enhances photosynthesis in the transgenic cyanobacterium, *Anabaena* PCC 7120. *J. Appl. Phycol.* **17,** 273–280 (2005).
56. Dejtisakdi, W. & Miller, S. M. Overexpression of Calvin cycle enzyme fructose-1,6-bisphosphatase in *Chlamydomonas reinhardtii* has a detrimental effect on growth. *Algal Res.* **14,** 116–126 (2016).
57. Tamoi, M., Nagaoka, M., Miyagawa, Y. & Shigeoka, S. Contribution of fructose-1,6-bisphosphatase and sedoheptulose-1,7-bisphosphatase to the photosynthetic rate and carbon flow in the Calvin cycle in transgenic plants. *Plant Cell Physiol.* **47,** 380–390 (2006).
58. Miyagawa, Y., Tamoi, M. & Shigeoka, S. Overexpression of a cyanobacterial fructose-1,6-/sedoheptulose-1,7-bisphosphatase in tobacco enhances photosynthesis and growth. *Nat. Biotechnol.* **19,** 965–969 (2001).
59. Ogawa, T. *et al.* Enhancement of photosynthetic capacity in Euglena gracilis by expression of cyanobacterial fructose-1,6-/sedoheptulose-1,7-bisphosphatase leads to increases in biomass and wax ester production. *Biotechnol. Biofuels.* **8,** 80 (2015).
60. Köhler, I. H. *et al.* Expression of cyanobacterial FBP/SBPase in soybean prevents yield depression under future climate conditions. *J. Exp. Bot.* **68,** 715–726 (2017).
61. Lefebvre, S. *et al.* Increased sedoheptulose-1,7-bisphosphatase activity in transgenic tobacco plants stimulates photosynthesis and growth from an early stage in development. *Plant Physiol.* **138,** 451–460 (2005).
62. Feng, L. *et al.* Overexpression of SBPase enhances photosynthesis against high temperature stress in transgenic rice plants. *Plant Cell Rep.* **26,** 1635–1646 (2007).
63. Rosenthal, D. M. *et al.* Over-expressing the C3 photosynthesis cycle enzyme Sedoheptulose-1-7-Bisphosphatase improves photosynthetic carbon gain and yield under fully open air CO_2 fumigation (FACE). *BMC Plant Biol.* **11,** 123 (2011).
64. Simkin, A. J. *et al.* Simultaneous stimulation of sedoheptulose-1,7-bisphosphatase, fructose-1,6-bisphophate aldolase and the photorespiratory glycine decarboxylase-H protein increases CO_2 assimilation, vegetative biomass and seed yield in *Arabidopsis*. *Plant Biotechnol. J.* **15,** 805–816 (2017).
65. Uematsu, K., Suzuki, N., Iwamae, T., Inui, M. & Yukawa, H. Increased fructose 1,6-bisphosphate aldolase in plastids enhances growth and photosynthesis of tobacco plants. *J. Exp. Bot.* **63,** 3001–3009 (2012).

66. Hatano-Iwasaki, a & Ogawa, K. Biomass production is promoted by increasing an aldolase undergoing glutathionylation in *Arabidopsis thaliana*. *Int. J. Plant Dev. Biol.* 1–8 (2012).
67. Yang, B. *et al.* Genetic engineering of the Calvin cycle toward enhanced photosynthetic CO_2 fixation in microalgae. *Biotechnol. Biofuels.* **10,** 229 (2017).
68. Khozaei, M. *et al.* Overexpression of plastid transketolase in tobacco results in a thiamine auxotrophic phenotype. *Plant Cell Online.* **27,** 432–447 (2015).
69. Suzuki, Y., Kondo, E. & Makino, A. Effects of co-overexpression of the genes of Rubisco and transketolase on photosynthesis in rice. *Photosynth. Res.* **131,** 281–289 (2017).
70. Ragsdale, S. W. & Pierce, E. Acetogenesis and the wood-ljungdahl pathway of CO_2 fixation. NIH Public Access. **1784,** 1873–1898 (2009).
71. Evans, M., Buchanan, B. & Arnon, D. A new ferredoxin-dependent carbon reduction cycle in a photosynthetic bacterium. *Proc. Natl. Acad. Sci. USA.* **55,** 928–934 (1966).
72. Herter, S., Fuchs, G., Bacher, A. & Eisenreich, W. A bicyclic autotrophic CO_2 fixation pathway in Chloroflexus aurantiacus. *J. Biol. Chem.* **277,** 20277–20283 (2002).
73. Berg, I. A., Kockelkorn, D., Buckel, W. & Fuchs, G. A 3-hydroxypropionate/4-hydroxybutyrate autotrophic carbon dioxide assimilation pathway in Archaea. *Science.* **318,** 1782–1786 (2007).
74. Huber, H. *et al.* A dicarboxylate/4-hydroxybutyrate autotrophic carbon assimilation cycle in the hyperthermophilic archaeum *Ignicoccus hospitalis*. *Proc. Natl. Acad. Sci. USA.* **105,** 7851–7856 (2008).
75. Claassens, N. J., Sousa, D. Z., Dos Santos, V. A. P. M., De Vos, W. M. & Van Der Oost, J. Harnessing the power of microbial autotrophy. *Nat. Rev. Microbiol.* **14,** 692–706 (2016).
76. Cotton, C. A., Edlich-Muth, C. & Bar-Even, A. Reinforcing carbon fixation: CO_2 reduction replacing and supporting carboxylation. *Curr. Opin. Biotechnol.* **49,** 49–56 (2018).
77. Figueroa, I. A. *et al.* Metagenomics-guided analysis of microbial chemolithoautotrophic phosphite oxidation yields evidence of a seventh natural CO_2 fixation pathway. *Proc. Natl. Acad. Sci. USA.* **115**, E92-E101 (2017).
78. Bar-Even, A. Formate Assimilation: The metabolic architecture of natural and synthetic pathways. *Biochemistry*. **55,** 3851–3863 (2016).
79. Bar-Even, A., Noor, E., Lewis, N. E. & Milo, R. Design and analysis of synthetic carbon fixation pathways. *Proc. Natl. Acad. Sci. USA.* **107,** 8889–8894 (2010).
80. Durall, C., Rukminasari, N. & Lindblad, P. Enhanced growth at low light intensity in the cyanobacterium *Synechocystis* PCC 6803 by overexpressing phosphoenolpyruvate carboxylase. *Algal Res.* **16,** 275–281 (2016).
81. Schwander, T., Schada von Borzyskowski, L., Burgener, S., Cortina, N. S. & Erb, T. J. A synthetic pathway for the fixation of carbon dioxide in vitro. *Science.* **354,** 900–904 (2016).
82. Gräslund, S. *et al.* Protein production and purification. *Nat. Methods.* **5,** 135–146 (2008).
83. Esposito, D. & Chatterjee, D. K. Enhancement of soluble protein expression through the use of fusion tags. *Curr. Opin. Biotechnol.* **17,** 353–358 (2006).

84. Butt, T. R., Edavettal, S. C., Hall, J. P. & Mattern, M. R. SUMO fusion technology for difficult-to-express proteins. *Protein Expr. Purif.* **43,** 1–9 (2005).
85. Malhotra, A. Tagging for Protein Expression. *Meth. Enzymol.* **463,** 239-258 (2009).
86. Smyth, D. & Mrozkiewicz, M. Crystal structures of fusion proteins with large affinity tags. *Protein Sci.* **12**, 1313–1322 (2003).
87. Waugh, D. S. Making the most of affinity tags. *Trends Biotechnol.* **23,** 316–320 (2005).
88. Puig, O. *et al.* The tandem affinity purification (TAP) method: A general procedure of orotein complex purification. *Methods.* **24,** 218–229 (2001).
89. Bucher, M. H., Evdokimov, A. G. & Waugh, D. S. Differential effects of short affinity tags on the crystallization of Pyrococcus furiosus maltodextrin-binding protein. *Acta Crystallogr. Sect. D Biol. Crystallogr.* **58,** 392–397 (2002).
90. Pajęcka, K. *et al.* Glutamate dehydrogenase isoforms with N-terminal (His)6- or FLAG-tag retain their kinetic properties and cellular localization. *Neurochem. Res.* **39,** 487–499 (2014).
91. Kosobokova, E. N., Skrypnik, K. A. & Kosorukov, V. S. Overview of fusion tags for recombinant proteins. *Biochem.* **81,** 187–200 (2016).
92. Leal, M. R. L. V., Walter, A. S. & Seabra, J. E. A. Sugarcane as an energy source. *Biomass Convers. Biorefinery*. **3,** 17–26 (2013).
93. Tilman, D. *et al.* Beneficial biofuels-the food, energy, and environment trilemma. *Science.* **325,** 270–271 (2009).
94. Wijffels, R. H. & Barbosa, M. J. An outlook on microalgal biofuels. *Science.* **329,** 796–799 (2010).
95. Du, W., Liang, F., Duan, Y., Tan, X. & Lu, X. Exploring the photosynthetic production capacity of sucrose by cyanobacteria. *Metab. Eng.* **19,** 17–25 (2013).
96. Abramson, B. W., Kachel, B., Kramer, D. M. & Ducat, D. C. Increased photochemical efficiency in cyanobacteria via an engineered sucrose sink. *Plant Cell Physiol.* **57,** 2451–2460 (2016).
97. Huang, H. H., Camsund, D., Lindblad, P. & Heidorn, T. Design and characterization of molecular tools for a synthetic biology approach towards developing cyanobacterial biotechnology. *Nucleic Acids Res.* **38,** 2577–2593 (2010).
98. Berla, B. M. *et al.* Synthetic biology of cyanobacteria: Unique challenges and opportunities. *Front. Microbiol.* **4,** 1–14 (2013).
99. Knoop, H. *et al.* Flux balance analysis of cyanobacterial metabolism: the metabolic network of *Synechocystis* sp. PCC 6803. *PLoS Comput. Biol.* **9,** 1–40 (2013).
100. Broddrick, J. T. *et al.* Unique attributes of cyanobacterial metabolism revealed by improved genome-scale metabolic modeling and essential gene analysis. *Proc. Natl. Acad. Sci. USA.* **113,** 8344–8353 (2016).
101. Yao, L., Cengic, I., Anfelt, J. & Hudson, E. P. Multiple gene repression in cyanobacteria using CRISPRi. *ACS Synth. Biol.* **5,** 207–212 (2016).
102. Wendt, K. E., Ungerer, J., Cobb, R. E., Zhao, H. & Pakrasi, H. B. CRISPR/Cas9 mediated targeted mutagenesis of the fast growing cyanobacterium *Synechococcus elongatus* UTEX 2973. *Microb. Cell Fact.* **15,** 115 (2016).
103. Orth, J. D., Thiele, I. & Palsson, B. Ø. What is flux balance analysis? *Nat Biotechnol.* **28,** 245–248 (2010).

104. O'Brien, E. J., Monk, J. M. & Palsson, B. O. Using genome-scale models to predict biological capabilities. *Cell.* **161,** 971–987 (2015).
105. Erdrich, P., Knoop, H., Steuer, R. & Klamt, S. Cyanobacterial biofuels: new insights and strain design strategies revealed by computational modeling. *Microb. Cell Fact.* **13,** 128 (2014).
106. Case, A. E. & Atsumi, S. Cyanobacterial chemical production. *J. Biotechnol.* **231,** 106–114 (2016).
107. Lindberg, P., Park, S. & Melis, A. Engineering a platform for photosynthetic isoprene production in cyanobacteria, using *Synechocystis* as the model organism. *Metab. Eng.* **12,** 70–79 (2010).
108. Bi, H., Wang, M., Dong, X. & Ai, X. Cloning and expression analysis of transketolase gene in Cucumis sativus L. *Plant Physiol. Biochem.* **70,** 512–521 (2013).
109. Ng, A. H., Berla, B. M. & Pakrasi, H. B. Fine-tuning of photoautotrophic protein production by combining promoters and neutral sites in the cyanobacterium *Synechocystis* sp. strain PCC 6803. *Appl. Environ. Microbiol.* **81,** 6857–6863 (2015).
110. Yeung, E. *et al.* The effect of compositional context on synthetic gene networks. *bioRxiv.* 1–35 (2016).
111. Englund, E., Andersen-Ranberg, J., Miao, R., Hamberger, B. & Lindberg, P. Metabolic engineering of *Synechocystis* sp. PCC 6803 for production of the plant diterpenoid manoyl oxide. *ACS Synth. Biol.* **4,** 1270–1278 (2015).
112. Garcia-Dominguez, M. *et al.* A gene cluster involved in metal homeostasis in the cyanobacterium *Synechocystis* sp. strain PCC 6803. *J. Bacteriol.* **182,** 1507–1514 (2000).
113. Miyawaki, a *et al.* Fluorescent indicators for Ca^{2+} based on green fluorescent proteins and calmodulin. *Nature.* **388,** 882–887 (1997).
114. Ducat, D. C., Avelar-Rivas, J. A., Way, J. C. & Silvera, P. A. Rerouting carbon flux to enhance photosynthetic productivity. *Appl. Environ. Microbiol.* **78,** 2660–2668 (2012).
115. Nocera, D. G. The artificial leaf. *Acc. Chem. Res.* **45,** 767–776 (2012).
116. Li, H. *et al.* Integrated electromicrobial conversion of CO_2 to higher alcohols. *Science.* **335,** 1596–1596 (2012).
117. Liu, C., Ziesack, M. & Silver, P. A. Water splitting-biosynthetic system with CO_2 reduction efficiencies exceeding photosynthesis. *Science.* **352**, 1210-1213 (2016)
118. Gagliardi, C. J. *et al.* Correction for Torella et al., Efficient solar-to-fuels production from a hybrid microbial–water-splitting catalyst system. *Proc. Natl. Acad. Sci. USA.* **112,** 2337-2342 (2015).
119. Li, Y.-J. *et al.* Engineered yeast with a CO_2-fixation pathway to improve the bio-ethanol production from xylose-mixed sugars. *Sci. Rep.* **7,** 43875 (2017).
120. Kirst, H., Formighieri, C. & Melis, A. Maximizing photosynthetic efficiency and culture productivity in cyanobacteria upon minimizing the phycobilisome light-harvesting antenna size. *BBA - Bioenerg.* **1837,** 1653–1664 (2014).
121. Gabilly, T., Niyogi, K. K. & Lemaux, P. G. Photosynthetic antenna engineering to improve crop yields. *Planta.* **245**, 1009–1020 (2017).
122. Erb, T. J., Jones, P. R. & Bar-even, A. Synthetic metabolism : metabolic engineering meets enzyme design. *Curr. Opin. Chem. Biol.* **37,** 56–62 (2017).

Acta Universitatis Upsaliensis

Digital Comprehensive Summaries of Uppsala Dissertations from the Faculty of Science and Technology 1616

Editor: The Dean of the Faculty of Science and Technology

A doctoral dissertation from the Faculty of Science and Technology, Uppsala University, is usually a summary of a number of papers. A few copies of the complete dissertation are kept at major Swedish research libraries, while the summary alone is distributed internationally through the series Digital Comprehensive Summaries of Uppsala Dissertations from the Faculty of Science and Technology. (Prior to January, 2005, the series was published under the title "Comprehensive Summaries of Uppsala Dissertations from the Faculty of Science and Technology".)

Distribution: publications.uu.se
urn:nbn:se:uu:diva-338081

ACTA
UNIVERSITATIS
UPSALIENSIS
UPPSALA
2018